

Spatiotemporal causal inference with arbitrary spillover and carryover effects*

Mitsuru Mukaigawara[†] Kosuke Imai[‡] Jason Lyall[§] Georgia Papadogeorgou[¶]

April 7, 2025

Abstract

Micro-level data with granular spatial and temporal information are becoming increasingly available to social scientists. Most researchers aggregate such data into a convenient panel data format and apply standard causal inference methods. This approach, however, has two limitations. First, data aggregation results in the loss of detailed geo-location and temporal information, leading to potential biases. Second, most panel data methods either ignore spatial spillover and temporal carryover effects or impose restrictive assumptions on their structure. We introduce a general methodological framework for spatiotemporal causal inference with arbitrary spillover and carryover effects. Under this general framework, we demonstrate how to define and estimate causal quantities of interest, explore heterogeneous treatment effects, investigate causal mechanisms, and visualize the results to facilitate their interpretation. We illustrate the proposed methodology through an analysis of airstrikes and insurgent attacks in Iraq. The open-source software package `geocausal` implements all of our methods.

Keywords: carryover effects, causal mechanisms, heterogeneous treatment effects, spatial point patterns, spillover effects

*All of the proposed methods can be implemented via an R package, `geocausal` (Mukaigawara et al., 2024), which is freely available for download at the [Comprehensive R Archive Network](https://comprarchive.org/). We thank the National Science Foundation for partial support (No. 2124124, 2124463, and 2124323). In addition, Imai acknowledges the Sloan Foundation (# 2020–13946) for financial support and Lyall gratefully acknowledges financial support from the Air Force Office of Scientific Research (Grant # FA9550-14-1-0072). The findings and conclusions reached here do not reflect the official views or policy of the United States Government or Air Force.

[†]Ph.D. Candidate, Department of Government, Harvard University, 1737 Cambridge Street, Cambridge MA, 02138. Email: mitsuru_mukaigawara@g.harvard.edu, URL: <https://www.mitsurumukaigawara.com>

[‡]Professor, Department of Government and Department of Statistics, Harvard University. 1737 Cambridge Street, Institute for Quantitative Social Science, Cambridge MA, 02138. Email: imai@harvard.edu, URL: <https://imai.fas.harvard.edu>

[§]James Wright Chair in Transnational Studies and Associate Professor, Department of Government, Dartmouth College, Hanover, NH 03755. Email: jason.lyall@dartmouth.edu, URL: <https://www.jasonlyall.com>

[¶]Assistant Professor, Department of Statistics, University of Florida, Gainesville FL 32603. Email: gpapadogeorgou@ufl.edu, URL: <https://gpapadogeorgou.netlify.com>

1 Introduction

Social scientists are increasingly leveraging the availability of micro-level data with spatial and temporal measurements. These data provide granular information about the locations and timing of various events. Examples include georeferenced data on political violence ([Sundberg and Melander, 2013](#); [Davies et al., 2024](#); [Raleigh, Kishi and Linke, 2023](#)), aid and development projects ([Sexton and Zürcher, 2024](#); [Harris and Posner, 2019](#)), natural disasters ([Young and Hsiang, 2024](#)), air pollution ([Monogan, Konisky and Woods, 2017](#)), and human mobility ([Aiken et al., 2022](#)).

Many existing studies, however, convert such data into a convenient panel data format so that they can apply standard causal inference methods. According to our literature review (see Appendix A), 80% of recently published papers in top political science journals, which analyze micro-level data, aggregate the data based on grid cells and administrative units ([Cox, Epp and Shepherd, 2024](#); [Crosson and Kaslovsky, 2024](#); [Bautista et al., 2023](#); [Lin, 2022](#); [Blair, 2024](#); [Sexton and Zürcher, 2024](#); [Sonin and Wright, 2024](#); [Muller-Crepon, 2024](#); [Cansunar, 2022](#); [Wood, 2014](#); [Polo and Welsh, 2024](#)). While the remaining papers use statistical methods that are designed to analyze spatial data, such as point process modeling and spatial smoothing and regressions, they do not estimate causal effects (e.g., [Cho and Gimpel, 2010](#); [Monogan, Konisky and Woods, 2017](#); [Harris and Posner, 2019](#)). Additionally, most studies model the spatial distribution of cross-sectional data without considering temporal variations.

Unfortunately, the methods used in the existing studies suffer from two major problems. First, data aggregation results in the loss of rich spatiotemporal information and possibly yield biased estimates. Many researchers choose units of analysis for convenience (e.g., district-month and grid-year), but this creates the potential sensitivity of empirical findings to the choice of aggregation units ([Zhukov et al., 2024](#)). Second, many researchers apply standard panel data analysis methods that either ignore spatial spillover and temporal carryover effects or impose restrictive assumptions on their structure (e.g., [Abadie, 2021](#); [Imai, Kim and Wang, 2023](#); [Xu, Zhao and Ding, 2024](#)). Such structural assumptions include restricting spillover effects to neighborhoods and limiting carryover effects to a small number of lags (e.g., [Sexton and Zürcher, 2024](#); [Christensen, 2019](#)). Yet, given how little we know about the nature of spillover and carryover effects, it is difficult to justify these assumptions in practice.

In this paper, we introduce a general causal inference methodology for spatiotemporal data with arbitrary spillover and carryover effects. The key advantage of the proposed methodology is that it directly models micro-level data without aggregating them and does not restrict the patterns of spillover and carryover effects. This means, for example, that spillover effects may not necessarily depend on physical distance alone while carryover effects may occur over time periods of various lengths across different locations. Given that many applications of spatiotemporal causal inference involve multiple events across space and over time, we focus on estimating the causal effects of changing the distribution of treatments rather than the separate causal effects of each treatment event. In other words, we analyze

how the outcome variable, which may also have both spatial and temporal dimensions, would change if we alter the spatial (and possibly temporal) distribution of treatments.

The proposed framework builds upon the general methodology developed in [Papadogeorgou et al. \(2022\)](#), which provides further technical details. We extend their methodology and show how to investigate causal mechanisms. While there exist a large methodological literature on causal mediation analysis (see [Imai et al., 2011](#); [Acharya, Blackwell and Sen, 2016](#); [VanderWeele, 2015](#), and references therein), the existing methods are unable to handle spatial and spatiotemporal data. We develop a new causal mediation analysis methodology that allows for arbitrary spillover and carryover effects. Finally, we also describe the estimation of heterogeneous treatment effects in the settings where the moderator, the treatment, and the outcome are all spatiotemporal (we leave the technical details to [Zhou et al. \(2024\)](#)). Again, the existing methods that estimate heterogeneous treatment effects are unable to deal with spatiotemporal variables (e.g., [Imai and Ratkovic, 2013](#); [Wager and Athey, 2018](#); [Künzel et al., 2019](#)). All together, the proposed methodology provides a set of tools necessary for causal inference with spatiotemporal data. We also develop an open-source software package `geocausal` with a detailed documentation so that other researchers are able to apply our methods to their own spatiotemporal causal inference ([Mukaigawara et al., 2024](#)).

Our proposed framework builds upon and extends the existing literature on spatiotemporal causal inference. A central challenge in spatiotemporal causal inference is unstructured interference, in which treatments may affect outcomes across arbitrary future time periods and spatial locations ([Wang et al., 2020](#)). Existing approaches have addressed this problem by either relying on design-based inference or imposing structural assumptions on spillover and carryover effects. For example, [Wang et al. \(2020\)](#) considers spatially randomized experiments in cross-sectional settings, assuming a finite set of potential intervention locations with known and fixed coordinates. Another common strategy involves imposing structural assumptions such as unit separation and aggregation (e.g., [Tchetgen Tchetgen, Fulcher and Shpitser, 2021](#)). In contrast, our framework addresses unstructured interference by representing treatments and outcomes as spatial point processes and employing stochastic interventions.

Despite the importance of effect heterogeneity and causal mechanisms, existing work on these problems in the spatiotemporal causal inference literature remains limited. Existing approaches to estimating heterogeneous treatment effects typically assume fixed interventions and a finite number of spatial units ([Zhang and Ning, 2023](#)). Prior mediation analysis methods in this context have either relied upon time-series of low-dimensional spatial summaries ([Runge et al., 2015](#)) or focused primarily on temporal (but not spatial) causal mediation ([Hizli et al., 2023](#)). Our framework advances this literature by enabling the analysis of effect heterogeneity and mediation under stochastic interventions.

To illustrate the proposed methodology, we investigate the effects of US airstrikes on insurgent violence during the Iraq War. We draw on declassified data from two sources — the US Air Force and

the Department of Defense — that record the date, location, and nature of US airstrikes and insurgent attacks with a high degree of geospatial precision. These data enable us to examine the causal effects of changing both the frequency and spatial distribution of airstrikes on subsequent insurgent attacks. We then explore possible effect heterogeneity of these airstrikes by considering how the presence and traits of US and UK forces, including their level of mechanization and density relative to district populations, might change how airstrikes condition insurgent violence. Finally, we turn to the question of causal mechanisms by exploring whether civilian casualties inflicted by these airstrikes mediate the overall relationship between airstrikes and insurgent attacks. Each topic has spawned a large literature. To date, however, they have been studied in isolation. Our framework, by contrast, integrates their study while acknowledging the importance of spillover and carryover effects that previous studies have ignored.

We find that US airstrikes increase, rather than deter or reduce, insurgent attacks. Moreover, we find that the escalatory effects of airstrikes are highest in areas that are occupied by more mechanized troops. There is a temporal dimension to this escalatory effect: increased insurgent attacks become apparent only after seven or more days of airstrikes. Contrary to conventional wisdom, the positive relationship between airstrikes and attacks is not mediated by civilian casualties. We find little evidence that airstrikes targeting civilian locations are more likely to generate insurgent violence than bombing military targets. Taken together, our findings suggest that insurgent attacks are motivated by a desire to demonstrate resolve by inflicting punishment on occupying forces rather than by revenge and grievances born from civilian harm.

The remainder of this paper is structured as follows. In Section 2, we introduce our motivating application and theory on the effects of airstrikes on insurgent attacks. In Section 3, we discuss the details of our proposed methodology. We then describe the causal assumptions and estimators in Section 4. The results of the analyses are presented in Section 5. We conclude in Section 6.

2 Airstrikes and insurgent activities in Iraq

Throughout this paper, we use a study of airstrikes and insurgent activities in Iraq as a motivating application. In this section, we first review theories and existing analyses related to the causal effects of airstrikes on insurgent activities. We then describe the micro-level data analyzed in our motivating application.

2.1 Debates surrounding the effects of airstrikes on insurgent activities

States have used airpower extensively in both interstate and counterinsurgency wars. One of such earliest examples is the Iraqi War of Independence in the 1920s (McDowall, 2000; Pape, 1996), in which the United Kingdom employed airstrikes against Iraqi insurgents. Recent counterinsurgency wars, such as those in Kosovo, Afghanistan, Somalia, Yemen, and Syria, also observed state actors' continuous reliance on airpower. In the past decade alone, the United States and its coalition reported 288 actions in

Somalia, 181 in Yemen, and 14,886 and 19,904 actions in Iraq and Syria, respectively (see the Airwars website at <https://airwars.org/>).

Despite the frequent use of airstrikes in counterinsurgency wars, scholars have yet to resolve three key debates surrounding the link between airstrikes and insurgent activities. First, the *effectiveness* of airstrikes in achieving strategic objectives is still uncertain. Some scholars argue that airstrikes have the potential to reduce insurgent activities through three mechanisms: decapitation, attrition, and punishment (Lyall, 2014; Pape, 1996). In contrast, others contend that airstrikes can increase insurgent activities through the mechanisms of grievances and the rebels' need to uphold their reputation for resolve (Condra and Shapiro, 2012; Kalyvas, 2006; Carr, 2003).

Second, another important debate is whether airstrikes have *heterogeneous effects* on insurgent attacks. While some studies explore heterogeneous effects in relation to aid (e.g., Kocher, Pepinsky and Kalyvas, 2011; Zhou et al., 2024; Dell and Querubin, 2018), it remains unclear whether troop characteristics, such as mechanization, troop densities, and the presence of certain troops, moderate the causal relationship between airstrikes and insurgent activities. Examining the moderating effect of troop characteristics is crucial for probing the mechanisms underlying the relationship between airstrikes and insurgent activity. Grievance-driven insurgents should target specific perpetrators like US forces, while those signaling resolve should focus on visible troops (Lyall, 2014). Moreover, understanding effect heterogeneity carries significant policy implications for developing strategies to mitigate insurgent attacks.

Lastly, it remains unclear if civilian casualties from airstrikes *mediate* insurgent activities. Airstrikes that deliberately or inadvertently kill civilians can coerce them into withdrawing support for the rebellion and refraining from joining it. However, such airstrikes can also generate grievances among civilians, increase support for insurgent organizations, and ultimately become counterproductive in counterinsurgency efforts (Kocher, Pepinsky and Kalyvas, 2011; Lyall, 2014). Such a contradictory prediction is not only theoretically critical, but also practically important because airstrikes almost always involve collateral damages of civilians. The direction and extent to which civilian casualties affect insurgent activities have thus garnered the attention of both scholars and practitioners (e.g., Condra and Shapiro, 2012; Condra et al., 2010; Kocher, Pepinsky and Kalyvas, 2011; Johnston and Sarbahi, 2016; Dell and Querubin, 2018; Lyall, 2014; Krick, Petkun and Revkin, 2023; Thier and Ranjbar, 2008). Several studies suggest that civilian casualties can lead to increased insurgent activities (e.g., Dell and Querubin, 2018; Condra and Shapiro, 2012), but other empirical analyses present mixed or opposing results (e.g., Condra et al., 2010; Lyall, 2014).

We will address these three debates by analyzing the causal relationships between airstrikes and insurgent activity during the Iraq War. Specifically, we develop and apply the methods that estimate the causal effects of airstrikes on insurgent attacks, explore heterogeneous treatment effects due to troop characteristics, and investigate the causal mechanisms based on civilian casualty. We now provide a brief

description of this motivating empirical application.

2.2 Motivating application

To illustrate our proposed methodology, we focus on the Iraq War (2003–11). The Iraq War is an important case for examining debates on airstrikes and insurgent activity, given the high number of civilian casualties. According to a study based on the Iraq Family Health Survey, an estimated 151,000 violent deaths occurred between March 2003 and June 2006 (Alkhuzai et al., 2008). The Iraq Body Count database (see <https://www.iraqbodycount.org/>), which compiles documented deaths, reports about 200,000 civilian fatalities to date. Additionally, the Iraq War is characterized by significant variation in troop composition. Multinational forces included troops from the United States, United Kingdom, and Australia, among others. Iraq’s diverse geography necessitated the involvement of both the Marine Corps and the Army.

We combine two declassified datasets to test the relationship between airstrikes, civilian casualties, and insurgent attacks. We first draw on the US Air Force’s own dataset of airstrikes and shows of force (simulated bombing runs) conducted in Iraq. These records include the date, aircraft type, and precise geographic coordinates (in Military Grid Reference System) of each air event along with information about the number and type of weapon released. We also use the Department of Defense’s Combined Information Data Network Exchange (CIDNE) dataset to measure insurgent attacks. CIDNE records the date, location (in MGRS), and type of insurgent attack, including Small Arms Fire (SAF) and Improvised Explosive Devices (IEDs), the two most frequent type of attack. We focus on the February 2007 to July 2008 time period, which captures the most intense fighting and subsequent sharp reduction of insurgent attacks during the so-called “Surge” of American forces to Iraq (Biddle, Friedman and Shapiro, 2012).

Given the precision of these data, we can use satellite imagery to classify the target of each airstrike. Pairing imagery with data on the blast radius of the ordinance dropped, we can capture a much more nuanced measure of civilian harm than simply counts of civilian fatalities. We categorize targets into eight broad groups: residential compounds, other buildings, farms, roads, settlements, unpopulated areas, unclassifiable areas, and others. We treat airstrikes on residential compounds and settlements as “civilian,” while roads and unpopulated areas, where strikes typically targeted insurgent bands, are treated as “military” in nature.¹

Finally, we use a micro-level dataset from Van Wie and Walden (2022b) to capture the location of US and UK military units in Iraq. This dataset provides weekly district-level data on dismount ratio (soldiers

¹We also cross-referenced all airstrikes with Iraq Body Count and newspaper searches for civilian casualties. Media reports typically underreport civilian casualties (Khan and Prickett, 2021; Khan, 2021; Khan and Gopal, 2017) due to access issues. Indeed, we find that only 3.5% of US airstrikes (112 of 3,159) are associated with civilian casualties during this time period. By contrast, our imagery indicates that civilian structures comprised more than 15% of targets struck. We therefore rely on our satellite imagery for our main analysis and replicate our findings using estimated civilian fatalities as a secondary measure.

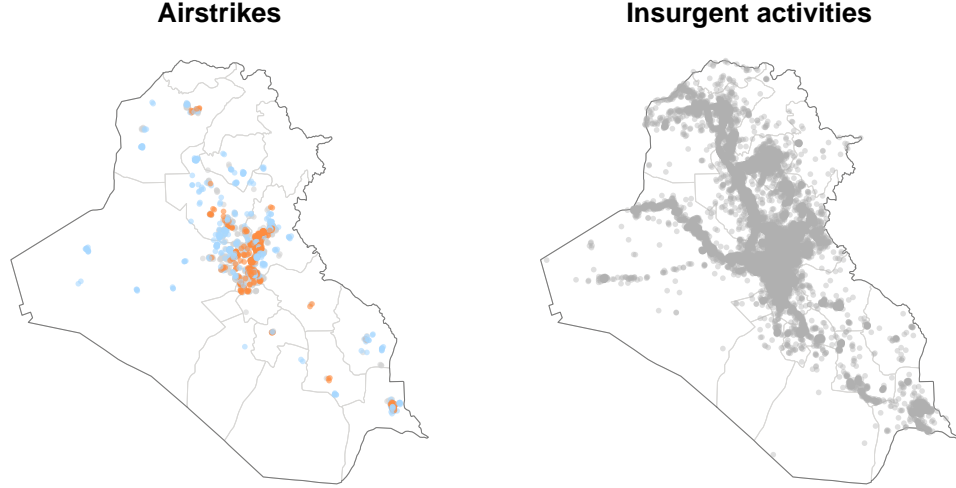


Figure 1: **Spatial distributions of airstrikes (left) and insurgent activities (right) in Iraq from February 2007 to July 2008.** For airstrikes (left), the orange, blue, and gray points represent airstrikes that hit civilian, military, and unclassifiable locations, respectively, based on satellite image classification.

per armored vehicle), troop density (soldiers per 1,000 residents), and indicator variables to denote the presence of US Marines or the UK Army instead of US Army units (the bulk of deployed forces).

Figure 1 illustrates the spatial distribution of airstrikes and insurgent attacks in Iraq between February 2007 and July 2008. The distributions are widespread across each administrative region of Iraq. In most regions, airstrikes are concentrated in a few locations, while leaving the majority of the region unaffected. This suggests that aggregating data at the administrative level not only leads to the loss of valuable information, but also introduces bias due to the neglect of spatial variations. We should also anticipate heterogeneous effects with respect to various local features. Additionally, insurgent attacks are more geographically dispersed, while airstrikes hitting civilians are concentrated in urban centers. This implies that the effect of civilian casualties on insurgent violence, if present, can manifest not only in the immediate vicinity of airstrike locations but also in more distant areas. This highlights the need for a methodology that accounts for long-range spillover effects of civilian casualties.

3 The proposed methodological framework

In this section, we introduce the proposed methodology for causal inference with spatiotemporal data. We first provide a key intuition about the concepts of spatial point processes and stochastic interventions, which play an essential role in our methodological framework. We then formally introduce the setup and define the causal estimands of interest for the overall effect estimation, heterogeneity analyses, and causal mediation analyses.

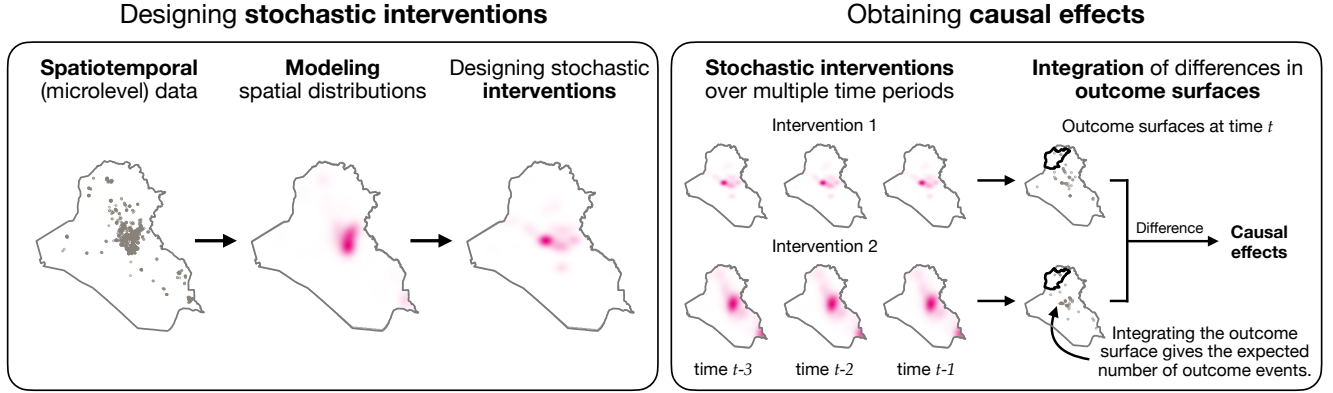


Figure 2: **Schematic summary of our spatiotemporal causal inference framework.** Stochastic interventions are designed based on the spatial distribution of the treatment. We then use them to estimate the causal effects of one intervention compared to another. We obtain the effect on the expected number of outcome events by taking the difference of integrated outcome surfaces.

3.1 Overview

Our methodology allows researchers to design granular spatiotemporal interventions and to make causal inference under arbitrary spillover and carryover effects. As illustrated in the left panel of Figure 2, the proposed framework begins with the following three steps: collecting spatiotemporal data, modeling the spatial distribution of treatments, and designing counterfactual stochastic interventions of interest by specifying their frequency, distribution, and duration. We use a spatial point process to model the spatial distribution of the treatment. For example, we use spatial and spatiotemporal covariates (including their lags) to model the treatment locations as an inhomogeneous Poisson point process, which allows treatment intensity to vary across locations (Baddeley, 2015). The expectation of this Poisson point process over a certain region of interest is the average number of treatment events occurring in that region.

Another key concept is stochastic intervention, which represents a hypothetical *distribution* of treatment events specified by researchers. The primary goal of our methodology is to estimate the counterfactual outcomes under this hypothetical stochastic intervention distribution. In our application, we use a counterfactual probability distribution of airstrikes across Iraq and over multiple time periods as a stochastic intervention. Researchers are free to choose this intervention distribution and it can be specified over multiple time periods, although selecting a distribution that is too different from the distributions of realized treatment events will lead to a high variance of the resulting causal estimates or even the violation of a key identification assumption.

After constructing counterfactual interventions, we investigate how the outcome events would occur if the treatment events were to arise from the specified hypothetical distribution. Intuitively, we view our treatment as a time-series of consecutive maps (or a single map if the stochastic intervention is specified

only for one period) that represent spatial distributions of treatment events. For example, one can employ a hypothetical distribution of airstrikes that are concentrated around Baghdad and apply it over three time periods (see Intervention 1 in the right panel of Figure 2). We might also consider another hypothetical intervention with a more widespread distribution of airstrikes (Intervention 2 of the same figure) and compare the outcomes under the two interventions.

As illustrated in the right panel of Figure 2, the proposed methodology estimates a counterfactual “outcome surface,” which represents a probability density of observing outcome events at every location in the space and at each time period under the specified hypothetical stochastic intervention, thereby allowing for arbitrary spillover and carryover effects. Averaging this outcome surface over time yields a variety of counterfactual quantities. For example, one can estimate the expected number of outcome events in a certain region under a counterfactual intervention of interest. Computing the differences in these counterfactual quantities under two stochastic interventions of interest lead to causal effect estimates.

Our approach does not require assumptions about spillover or carryover effects. To design hypothetical interventions, we avoid segmenting the entire geographical area of interest into regions such as districts and grid cells. Instead, we define our interventions as probability distributions of treatment events across the entire space over multiple time periods. Additionally, our methodology can estimate the outcome surface at each subsequent period after a stochastic intervention without restricting the range of carryover effects.

3.2 Setup

We now formally present the proposed methodology. Let Ω represent the entire geographical region of interest. We denote time periods with $t = 1, 2, \dots, T$ where T represents the total number of time periods. In our application, Ω is the entire country of Iraq and $T = 499$ (in days). At each time period, the treatment assignment is a spatial point pattern over Ω . We define the binary treatment variable at each location $s \in \Omega$ as $W_t(s)$, which indicates whether the location received the treatment ($W_t(s) = 1$) or not ($W_t(s) = 0$) at time period t . The collection of $W_t(s)$ at all locations fully represents the treatment point pattern at time period t and is denoted by the random variable $W_t = \{W_t(s), s \in \Omega\}$ with its realization w_t . Alternatively, the treatment point pattern can be fully represented through the locations that received the treatment, referred to as the *treatment active locations* and denoted by $S_{W_t} = \{s \in \Omega : W_t = 1\}$. In our setting, S_{W_t} represents the airstrike locations in Iraq on the t th day. Lastly, we denote the treatment history by $\overline{\mathbf{W}}_t = (W_1, W_2, \dots, W_t)$ and its realization by $\overline{\mathbf{w}}_t = (w_1, \dots, w_t)$.

Next, let Y_t denote the observed outcome point pattern at time t where $Y_t(s) = 1$ if location s experiences the outcome event at that time and $Y_t(s) = 0$ if it does not. In our application, $Y_t(s) = 1$ if location s observes insurgent attacks at time t . For a given treatment history $\overline{\mathbf{w}}_t$, we denote the corresponding potential outcome by $Y_t(\overline{\mathbf{w}}_t)$ and the observed outcome by $Y_t = Y_t(\overline{\mathbf{W}}_t)$, respectively.

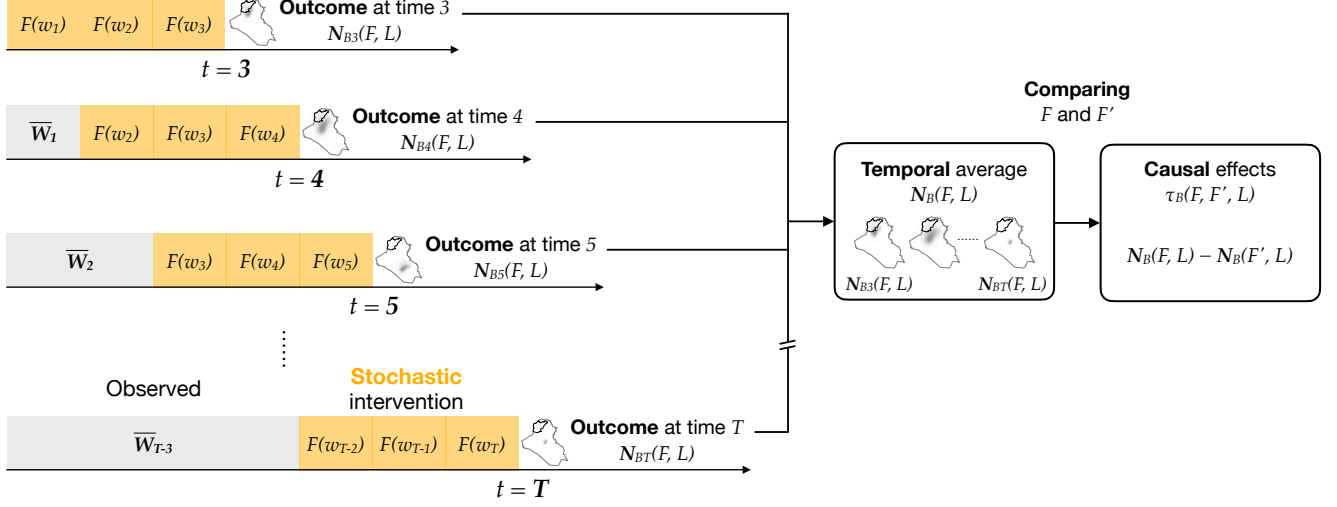


Figure 3: **Schematic representation of the causal estimands.** The estimand $N_{Bt}(F, L)$ represents the expected number of outcome active locations given a stochastic intervention F over preceding L time periods (shown in orange). For illustrative purposes, we set $L = 3$. Treatment histories are fixed prior to intervention F (shown in gray). The estimand $N_B(F, L)$ represents the temporal average of $N_{Bt}(F, L)$ across $t = 3, \dots, T$. The difference between $N_B(F, L)$ and $N_B(F', L)$ represents the temporal average effects of switching from intervention F' to F .

We use $\mathcal{Y}_{\mathcal{T}} = \{Y_t(\bar{w}_t), \text{ for all } t \text{ and } \bar{w}_t\}$ to denote the collection of all potential outcomes under any treatment path and for any time point. We use $\bar{\mathbf{Y}}_t = \{Y_1, Y_2, \dots, Y_t\}$ to represent the observed outcomes up to time t .

Finally, we use \mathbf{X}_t to denote a collection of spatiotemporal confounders at time t that are causally prior to the realized treatment for the same time period, i.e., W_t . These confounders can be either time-varying or time-invariant, and may or may not vary across space. Furthermore, the confounders may be arbitrarily affected by the past treatment history. Therefore, we let $\mathbf{X}_t(\bar{w}_{t-1})$ denote the potential value of the confounders at time period t that would result for a given treatment history. Then, the observed confounders are represented by $\mathbf{X}_t = \mathbf{X}_t(\bar{\mathbf{W}}_{t-1})$, and the history of observed confounders are represented by $\bar{\mathbf{X}}_t = (\mathbf{X}_1, \mathbf{X}_2, \dots, \mathbf{X}_t)$. We use $\mathcal{X}_{\mathcal{T}}$ to denote the collection of all potential confounder values for all time points, similarly to $\mathcal{Y}_{\mathcal{T}}$. We use $\bar{H}_t = \{\bar{\mathbf{W}}_t, \bar{\mathbf{Y}}_t, \bar{\mathbf{X}}_{t+1}\}$ to denote the observed random variables that have occurred up until the treatment assignment at time period $t + 1$.

3.3 Average treatment effects

Our causal estimands are based on the expected number of outcome events at each time period t in a certain region $B \subset \Omega$ under a specified stochastic intervention F that lasts during L time periods with $L \geq 1$. Since we treat the data as a time-series of maps, the causal estimand is defined by averaging the expected number of outcome events over the $T - L + 1$ time periods (we set aside the first $L - 1$ time periods, which correspond to the periods of stochastic intervention).

Figure 3 provides a schematic summary of how we define the average treatment effects. For illustrative purposes, we consider a stochastic intervention F that lasts for $L = 3$ time periods (shown in orange). For each time period $t = 3, \dots, T$, we compute the expected number of outcome events under this intervention in region B , conditional on observed airstrikes up to time $t - L$, i.e., $\overline{\mathbf{W}}_{t-L}$. These expected count measures $\mathbf{N}_{Bt}(F, L)$ are obtained by integrating the counterfactual outcome surface over the region. In the current example, we generate a total of $T - L + 1 = T - 2$ expected outcomes: $\mathbf{N}_{B3}(F, L), \dots, \mathbf{N}_{BT}(F, L)$. We then take the temporal average of all $\mathbf{N}_{Bt}(F, L)$ for $t = 3, \dots, L$ and obtain a spatially and temporally averaged outcome, $\mathbf{N}_B(F, L)$ (the center box in the figure). Lastly, to compare the effects of intervention F relative to another intervention F' , we take the difference between $\mathbf{N}_B(F, L)$ and $\mathbf{N}_B(F', L)$, resulting in the average treatment effect $\tau_B(F, F', L)$ shown in the right box.

Formally, we follow [Papadogeorgou et al. \(2022\)](#) and define the expected number of outcome events in region B at time period t under stochastic intervention F as follows:

$$\mathbf{N}_{Bt}(F, L) = \int_{\mathcal{W}} \cdots \int_{\mathcal{W}} N_B(Y_t(\overline{\mathbf{W}}_{t-L}, w_{t-L+1}, \dots, w_t)) dF(w_{t-L+1}) \cdots dF(w_t), \quad (1)$$

where $N_B(\cdot)$ counts the number of outcome events within B , and \mathcal{W} denotes the set of all possible treatment active locations at each period. Equation (1) integrates the counterfactual outcome surface with respect to the stochastic intervention F over L time periods. In our application, $\mathbf{N}_{Bt}(F, L)$ represents the expected number of insurgent attacks under a stochastic intervention of airstrikes F over L time periods.

Once $\mathbf{N}_{Bt}(F, L)$ is defined for each time period, we further average it over time to obtain the expected number of outcome events in region B . Averaging over time as well as space is essential because the uncertainty of a single observation $\mathbf{N}_{Bt}(F, L)$ cannot be directly assessed. Formally, our primary causal estimand is given by:

$$\mathbf{N}_B(F, L) = \frac{1}{T - L + 1} \sum_{t=L}^T \mathbf{N}_{Bt}(F, L) \quad (2)$$

where temporal averaging starts from $t = L$ given that the stochastic intervention F is defined over L time periods. Finally, we can define the average effect of a stochastic intervention F relative to another intervention F' (i.e., average treatment effect or ATE) as,

$$\tau_B(F, F', L) = \mathbf{N}_B(F, L) - \mathbf{N}_B(F', L). \quad (3)$$

3.4 Heterogeneous treatment effects

In addition to the ATE, researchers are often interested in characterizing the treatment effects as functions of certain moderators. In causal inference with spatiotemporal data, we examine how the treatment

effect at each small geographical area, which we refer to as “pixel”, vary as a function of its spatial or spatiotemporal characteristics. Specifically, we first partition Ω into p disjoint regions and then define the pixel-level conditional average treatment effect (CATE) using its spatial or spatiotemporal characteristics. Finally, we compute the average of these pixel-level CATEs across pixels with the same moderator value (Zhou et al., 2024). Since the moderator may take many different values, we use linear projection to summarize the relationship between pixel-level CATEs and the moderator variable.

Formally, let $\mathcal{Q} = \{Q_1, \dots, Q_p\}$ be the set of p non-overlapping small geographical regions (i.e., pixels) that consist of Ω , where $\Omega = \cup_{i=1}^p Q_i$ and $Q_i \cap Q_{i'} = \emptyset$ for $i \neq i'$. We use $\mathbf{R}_{it} \in \mathcal{R}$ to denote the vector-value of the potential moderator in pixel S_i at time t , with \mathcal{R} representing the support of the moderator. The value \mathbf{R}_{it} should be constant within Q_i at time t . If the moderator is not constant within each pixel at any given time period, then we can use a summary statistic such as the mean. In our application, \mathbf{R}_{it} represents troop characteristics, including mechanization, troop density, and the presence of the British Armed Forces or the US Marine Corps.

Given this setup, we first define the pixel-level CATE by applying Equation (1) to pixel Q_i as follows:

$$\mathbf{N}_{it}(F, L) = \int_{\mathcal{W}} \cdots \int_{\mathcal{W}} N_{Q_i} \left(Y_t(\overline{\mathbf{W}}_{t-L}, w_{t-L+1}, \dots, w_t) \right) dF(w_{t-L+1}) \cdots dF(w_t).$$

Then, the difference in the pixel-level CATE between two stochastic interventions is given by:

$$\tau_{it}(F', F'', L) = \mathbf{N}_{it}(F', L) - \mathbf{N}_{it}(F'', L). \quad (4)$$

We can now define the overall CATE by taking the average of Equation (4) over all pixels with the same moderator value $\mathbf{r} \in \mathcal{R}$:

$$\tau_t(F', F'', L; \mathbf{r}) = \frac{1}{\sum_{i=1}^p I(\mathbf{R}_{i,t-L+1} = \mathbf{r})} \sum_{i=1}^p \tau_{it}(F', F'', L) I(\mathbf{R}_{i,t-L+1} = \mathbf{r}), \quad (5)$$

where I represents the indicator function. In Equation (4), we use the moderator value measured at time $t - L + 1$, which is immediately before the application of stochastic interventions. This ensures that the moderator is unaffected by the treatment and therefore avoids post-treatment bias.

An important limitation of the CATE defined in Equation (5) is that the moderator may take many values, resulting in a small number of observations for each unique value of $\mathbf{R}_{i,t-L+1}$. This results in an imprecise estimate of the CATE function. To address this problem, we summarize the relationship between the treatment effects and the moderator values by projecting the former onto the latter. One simple example of such projection is linear regression where we regress $\tau_t(F', F'', L; \mathbf{R}_{i,t-L+1})$ on $\mathbf{R}_{i,t-L+1}$. We can also use a nonparametric method such as local linear regression.

Formally, we define the time-specific projection estimand $\tilde{\tau}_t(F', F'', L; \mathbf{R}_{t-L+1}, \boldsymbol{\beta}_t^*)$, where

$$\boldsymbol{\beta}_t^* = \arg \min_{\boldsymbol{\beta}_t} \sum_{i=1}^p (\tau_t(F', F'', L; \mathbf{R}_{i,t-L+1}) - \tilde{\tau}_t(F', F'', L; \mathbf{R}_{i,t-L+1}, \boldsymbol{\beta}_t))^2 \quad (6)$$

with the following projection model that minimizes the mean square error,

$$\tilde{\tau}_t(F', F'', L; \mathbf{r}, \boldsymbol{\beta}_t) = \sum_{k=1}^K \beta_{tk} z_k(\mathbf{r}) = \mathbf{z}(\mathbf{r})^\top \boldsymbol{\beta}_t$$

with known functions $\mathbf{z}(\mathbf{r}) = [z_1(\mathbf{r}), \dots, z_K(\mathbf{r})]^\top$. In the case of linear regression, we have $z_k(\mathbf{r}) = \mathbf{r}$ and $K = 1$. Therefore, the above projection model represents the best approximation of the CATE using the moderator. Finally, the overall CATE is defined as the average of time-specific CATEs over time periods $L, L+1, \dots, T$,

$$\tilde{\tau}(F', F'', L; \mathbf{r}, \boldsymbol{\beta}_L^*, \dots, \boldsymbol{\beta}_T^*) = \frac{1}{T-L+1} \sum_{t=L}^T \tilde{\tau}_t(F', F'', L; \mathbf{R}_{i,t-L+1} = \mathbf{r}, \boldsymbol{\beta}_t^*).$$

3.5 Causal mediation analysis

Researchers often explore causal mechanisms and examine how the treatment affects an outcome through certain mediators (Imai et al., 2011). Below, we develop a methodology for causal mediation analysis with spatiotemporal data. Like the treatment variable, our mediator variable is a stochastic intervention based on point patterns. We first modify notation to incorporate a mediator. Let $M_t(s) \in \mathcal{M}$ represent the mediating variable at location $s \in \Omega$ where \mathcal{M} is its support. In our application, $M_t(s)$ is a categorical variable since it represents the different types of airstrike locations (e.g., residential, farm land). For the sake of simplicity, we consider a binary mediator $M_t(s) \in \mathcal{M} = \{0, 1\}$ that indicates the presence of civilian casualty; later we will consider a more nuanced, categorical mediator. Like the treatment variable, we use M_t to represent the collection of mediator values at all locations, $M_t = \{M_t(s), s \in \Omega\}$ with its realization denoted by m_t . In addition, the collection of *mediator active locations* is denoted by $S_{M_t} = \{s \in \Omega : M_t(s) \neq 0\}$, while the mediator history is represented by $\overline{\mathbf{M}}_t = (M_1, M_2, \dots, M_t)$ with its realization $\overline{\mathbf{m}}_t$. Hence, airstrike locations with civilian casualty are both *treatment active* and *mediator active* locations. In contrast, locations with airstrikes that did not kill civilians are *treatment active* but not *mediator active* locations.

We next define the potential and observed values of the mediators. In its full generality, let $M_t(\overline{\mathbf{w}}_t, \overline{\mathbf{m}}_{t-1})$ denote the value of the mediator we would observe at time period t , had previous treatment and mediator histories been equal to $\overline{\mathbf{w}}_t$ and $\overline{\mathbf{m}}_{t-1}$, respectively.² In addition, let $M_t(\overline{\mathbf{w}}_t, \overline{\mathbf{m}}_{t-1}; s)$ be its value

²Since the mediator value is realized after the treatment at time t , M_t is a function of $\overline{\mathbf{w}}_t$ rather than $\overline{\mathbf{w}}_{t-1}$.

at location $s \in \Omega$. This definition allows for the mediator to be affected by all past treatments and mediator values at any location, highlighting the fact that our methodology allow for arbitrary spillover and carryover effects. Lastly, we assume that the observed mediator equals its potential value for the observed path, i.e., $M_t = M_t(\overline{\mathbf{W}}_t, \overline{\mathbf{M}}_{t-1})$. Although our methodology can handle more general cases, here we focus on the setting, in which all mediator active locations are also treatment active locations, i.e., $\{s \in \Omega : M_t(\overline{\mathbf{w}}_t, \overline{\mathbf{m}}_{t-1}; s) \neq 0\} \subset \{s \in \Omega : w_t(s) \neq 0\}$ for all $\overline{\mathbf{w}}_t$ and $\overline{\mathbf{m}}_{t-1}$. In our application, this restriction holds because airstrike-caused civilian casualties are our mediator, and civilian casualties can occur only at airstrike locations.

We can now define the potential and observed values of outcomes and confounders. For a given treatment and mediator history, $(\overline{\mathbf{w}}_t, \overline{\mathbf{m}}_t) = (w_1, m_1, \dots, w_t, m_t)$, we denote the corresponding potential outcome by $Y_t(\overline{\mathbf{w}}_t, \overline{\mathbf{m}}_t)$ and the observed outcome by $Y_t = Y_t(\overline{\mathbf{W}}_t, \overline{\mathbf{M}}_t)$, respectively. We use $\mathcal{Y}_{\mathcal{T}} = \{Y_t(\overline{\mathbf{w}}_t, \overline{\mathbf{m}}_t), \text{ for all } t, \overline{\mathbf{w}}_t, \text{ and } \overline{\mathbf{m}}_t\}$ to denote the collection of all potential outcomes under any treatment and mediator path and for any time point. Additionally, we let $\mathbf{X}_t(\overline{\mathbf{w}}_{t-1}, \overline{\mathbf{m}}_{t-1})$ denote the potential value of the confounders at time period t that would result for a given treatment and mediator history. Then, the observed confounders are represented by $\mathbf{X}_t = \mathbf{X}_t(\overline{\mathbf{W}}_{t-1}, \overline{\mathbf{M}}_{t-1})$, while the history of observed confounders is denoted by $\overline{\mathbf{X}}_t = (\mathbf{X}_1, \mathbf{X}_2, \dots, \mathbf{X}_t)$. We use $\mathcal{X}_{\mathcal{T}}$ to denote the collection of all potential confounder values for all time points, similarly to $\mathcal{Y}_{\mathcal{T}}$. We use $\overline{H}_t = \{\overline{\mathbf{W}}_t, \overline{\mathbf{M}}_t, \overline{\mathbf{Y}}_t, \overline{\mathbf{X}}_{t+1}\}$ to denote the observed random variables that have occurred up until the treatment assignment at time period $t + 1$.

Given this new setup with a mediator, we now define our causal estimands. To do so, we specify the conditional distribution of the mediator given the treatment as another stochastic intervention in addition to a stochastic intervention of the treatment variable. Formally, let F_W denote an intervention distribution that generates the treatment variable W_t independently in each of L subsequent time periods. We also specify the conditional distribution of mediator given the treatment, $F_{M|w}$, which would be applied over the same L time periods. We now refer to the pair $F = (F_W, F_{M|w})$ as stochastic intervention over (W, M) , and use $F(w, m)$ to denote the joint distribution $F_W(w)F_{M|w}(m)$. We can then redefine the expected number of outcome events given in Equation (1) by incorporating mediators as follows:

$$N_{Btm}(F, L) = \int_{(\mathcal{W}, \mathcal{M})} \dots \int_{(\mathcal{W}, \mathcal{M})} N_B\left(Y_t(\overline{\mathbf{W}}_{t-L}, \overline{\mathbf{M}}_{t-L}, w_{t-L+1}, m_{t-L+1}, \dots, w_t, m_t)\right) dF(w_{t-L+1}, m_{t-L+1}) \dots dF(w_t, m_t). \quad (7)$$

Similarly to Equation (1), the distributions of both the treatment and mediator are fixed until time $t - L$ to their observed values, i.e., $\overline{\mathbf{W}}_{t-L}$ and $\overline{\mathbf{M}}_{t-L}$. For the remaining time periods from $t - L + 1$ to t , we employ stochastic intervention $F(w, m)$ for the treatment and mediator variables.

Just like $N_{Bt}(F, L)$ in Equation (1), the estimand $N_{Btm}(F, L)$ needs to be averaged over time:

$$N_{Bm}(F, L) = \frac{1}{T - L + 1} \sum_{t=L}^T N_{Btm}(F, L).$$

To compare the effects of stochastic interventions $F' = (F'_W, F'_{M|w})$ and $F'' = (F''_W, F''_{M|w})$, we consider the difference between the two stochastic interventions by,

$$\tau_{Bm}(F', F'', L) = N_{Bm}(F'', L) - N_{Bm}(F', L).$$

A key benefit of causal mediation analysis is its ability to decompose total effects into direct and indirect treatment effects (Imai et al., 2011). In the current setup, direct effects capture the effects of changing the treatment distribution while fixing the mediator distribution, whereas indirect effects represent the effects of changing the mediator distribution while holding the treatment distribution constant. Formally, we define the *direct effect* of altering the treatment intervention distribution from F'_W to F''_W while keeping the mediator distribution unchanged as $F_{M|w}$ by,

$$\tau_{Bm}^{DE}(F'_W, F''_W; L, F_{M|w}) = \tau_{Bm}((F'_W, F_{M|w}), (F''_W, F_{M|w}), L). \quad (8)$$

Similarly, the corresponding *indirect effect* is defined by fixing the treatment intervention as F_W and changing the mediator distribution from $F'_{M|w}$ to $F''_{M|w}$:

$$\tau_{Bm}^{IE}(F'_{M|w}, F''_{M|w}; L, F_W) = \tau_{Bm}((F_W, F'_{M|w}), (F_W, F''_{M|w}), L). \quad (9)$$

In our application, direct effects represent the effects of altering the distribution of airstrikes while keeping the conditional distribution of civilian casualties fixed. Similarly, indirect effects represent the effects of changing civilian casualties while fixing the airstrike distribution. As in the standard mediation analysis, these direct and indirect effects sum to the total effect; there are two decompositions, depending on which intervention distribution is held constant. But, the difference is that total effects represent the effects of changing both treatment and mediator stochastic interventions.

$$\begin{aligned} \tau_{Bm}(F', F'', L) &= \tau_{Bm}^{IE}(F'_{M|w}, F''_{M|w}; L, F'_W) + \tau_{Bm}^{DE}(F'_W, F''_W; L, F'_{M|w}) \\ &= \tau_{Bm}^{IE}(F'_{M|w}, F''_{M|w}; L, F''_W) + \tau_{Bm}^{DE}(F'_W, F''_W; L, F'_{M|w}). \end{aligned}$$

The direct and indirect effects enable the exploration of the causal mechanisms of airstrikes while accounting for complex spatial spillover effects. For example, we may expect an airstrike that kills more civilians to generate more attacks by insurgents who may try to establish their dominance in the bombed

area. We can test this hypothesis by estimating the indirect effect $\tau_{Bm}^{\text{IE}}(F'_{M|w}, F''_{M|w}; L, F_W)$ where we specify $F''_{M|w}$ such that it generates a greater number of civilian casualties than $F'_{M|w}$.

4 Estimation

In this section, we introduce the estimators for the ATE, heterogeneous effects, and causal mediation effects. We first discuss two essential causal assumptions required for the estimation of the ATE and heterogeneous treatment effects. They are versions of the unconfoundedness and overlap assumptions that are commonly required in standard causal inference settings. We show that under these assumptions, the proposed estimators are consistent and asymptotically normal. Finally, we extend the causal assumptions by accommodating the presence of mediators, develop the estimators for direct, indirect, and total effects in causal mediation analysis, and derive their asymptotic properties.

4.1 Average treatment effects

We begin by introducing two causal assumptions. We first consider the unconfoundedness assumption, which ensures that the treatment assignment is random given the observed covariates (Papadogeorgou et al., 2022; Bojinov and Shephard, 2019). Formally, let f denote the density of intervention F . The unconfoundedness assumption in our context is stated as follows.

Assumption 1 (Unconfoundedness). *The treatment assignment at time t does not depend on any unobserved potential outcomes or potential values for the time-varying confounders given the observed history:*

$$f(W_t | \overline{\mathbf{W}}_{t-1}, \overline{\mathcal{Y}}_T, \overline{\mathcal{X}}_T) = f(W_t | \overline{H}_{t-1}).$$

Assumption 1 states that the realized assignment of the treatment point patterns at time period t is conditionally independent of *both past and future* potential outcomes and confounders, given the observed history. Therefore, Assumption 1 is more restrictive than the standard sequential ignorability assumption (Robins, Hernan and Brumback, 2000), which requires the conditional independence with respect to future potential outcomes alone.

We next consider the overlap assumption. We need the overlap assumption because the hypothetical treatment patterns under the stochastic intervention should be sufficiently likely to be observed with non-zero probabilities. Formally, the overlap assumption in our context is given as follows.

Assumption 2 (Bounded relative overlap). *The density ratio between the treatment point pattern of the realized data and that of the hypothetical intervention is bounded, i.e., there exists a positive constant δ such that*

$$\frac{f(w | \overline{H}_{t-1})}{f(w)} > \delta$$

for all $w \in \mathcal{W}$.

Under these assumptions, we now introduce the ATE estimator by extending the inverse probability of treatment weighting estimator to spatiotemporal point pattern data. Intuitively, our estimator represents

a *weighted average of spatially-smoothed outcomes*. The weights represent the ratio of the intervention density over the propensity score evaluated with the observed outcome. In other words, the weights show how likely it is to observe the realized treatment events under a stochastic intervention relative to the propensity score. This approach avoids direct outcome modeling, thereby circumventing the need to accurately specify spillover or carryover effects.

Formally, we define the weight of time period t according to intervention F as

$$\zeta_t(F, L) = \prod_{t'=t-L+1}^t \frac{f(W_{t'})}{e_{t'}(W_{t'})}, \quad (10)$$

where the weight is the product of L ratios because the stochastic intervention is defined over L time periods. Each ratio in the product represents the relative likelihood of observing the realized treatment at each time period under the hypothetical intervention over the propensity score.

Second, we define a spatially-smoothed version of the outcome response. Smoothing is often necessary because spatiotemporal data tend to be sparse. This means that in many regions of interest the number of observed outcome events may not be large, resulting in an inefficient estimator. To borrow strength from neighboring regions, we use kernel smoothing on the observed point pattern and obtain the smoothed outcome surface at time point t ,

$$\tilde{Y}_t(\omega) = \sum_{s \in S_{Y_t}} K_b(\|\omega - s\|), \quad \omega \in \Omega, \quad (11)$$

where $K_b(u) = b^{-1}K(u/b)$ is a kernel with bandwidth parameter b and $\|\cdot\|$ is the Euclidean norm (i.e., spatial distance). Intuitively, the value of the smoothed outcome surface at a point ω is the weighted sum of densities evaluated at all outcome active locations with the weights inversely proportional to their distance from ω . The bandwidth b controls the degree of smoothing with a greater value indicating a less smooth surface.³

We now combine the weights $\zeta_t(F, L)$ and the smoothed outcome surface $\tilde{Y}_t(\omega)$ to define the weighted smoothed outcome surface $\hat{Y}_t : \Omega \rightarrow \mathbb{R}^+$ as

$$\hat{Y}_t(F, L; \omega) = \zeta_t(F, L) \tilde{Y}_t(\omega). \quad (12)$$

The integral of this weighted smoothed outcome surface over a region of interest B estimates the expected number of points within that region under the stochastic intervention. Specifically, we define the

³We can think of K_b as a scaled version of a kernel $K : [0, \infty) \rightarrow [0, \infty)$ with $\int K(u)du = 1$, where K is a smooth function used to estimate the spatial spread patterns of insurgent attacks. Therefore, $K_b(u)$ adjusts the spread of outcomes based on the bandwidth b .

estimator of $N_{Bt}(F, L)$ (see Equation (1)) and its temporal average $N_B(F, L)$ (see Equation (2)) as,

$$\widehat{N}_{Bt}(F, L) = \int_B \widehat{Y}_t(F, L; \omega) d\omega, \quad (13)$$

$$\widehat{N}_B(F, L) = \frac{1}{T - L + 1} \sum_{t=L}^T \widehat{N}_{Bt}(F, L). \quad (14)$$

Then, the estimator of the ATE $\tau_B(F', F'', L)$ (see Equation (3)) is defined as

$$\widehat{\tau}(F', F'', L) = \widehat{N}_B(F'', L) - \widehat{N}_B(F', L). \quad (15)$$

Papadogeorgou et al. (2022) show that these estimators are consistent and asymptotically normal.

As we have shown in Equation (10), our estimators are inverse probability weighting (IPW) estimators because we divide the stochastic intervention density $f(W_{t'})$ by the propensity score $e_{t'}(W_{t'})$. These IPW estimators become unstable if the propensity scores are too small. To address this issue, we also employ the Hájek estimator, which stabilizes the weights $\zeta_t(F, L)$ through normalization (so that the sum of weights is one). To employ the Hájek estimator, we can replace Equation (14) with,

$$\widehat{N}_B(F, L) = \sum_{t=L}^T \widehat{N}_{Bt}(F, L) / \sum_{t=L}^T \zeta_t(F, L).$$

Zhou et al. (2024) shows that this Hájek estimator is consistent and asymptotically normal.

4.2 Heterogeneous treatment effects

The intuition behind the estimation strategy for heterogeneous treatment effects is illustrated in Figure 4. The estimation strategy consists of two steps. In the first step, we estimate the causal effects in each pixel (Figure 4, left, shown as blue pixel-level grid cells). This procedure is similar to ATE estimation but is conducted at the pixel level. We then consider the value of the moderator in each pixel (Figure 4, left, shown as green pixel-level grid cells). Spatially continuous moderators (e.g., population density, terrain features) need to be summarized at the pixel level to ensure that each pixel has a single moderator value. For discrete moderators that already have one value per pixel, this step can be omitted.

In the second step, we fit a time-specific regression for each time period (Figure 4, right). Specifically, for each time period t , we regress pixel-level treatment effects on pixel-level moderator values from the pre-intervention period (time $t - L + 1$). By performing this image-to-image regression, we project treatment effects onto moderator values. This projection step is crucial because, given the wide range of possible moderator values, simply averaging pixel-level treatment effects by moderator values could lead to imprecise estimates.

To estimate heterogeneous treatment effects, we continue to rely on Assumptions 1 and 2. Formally,

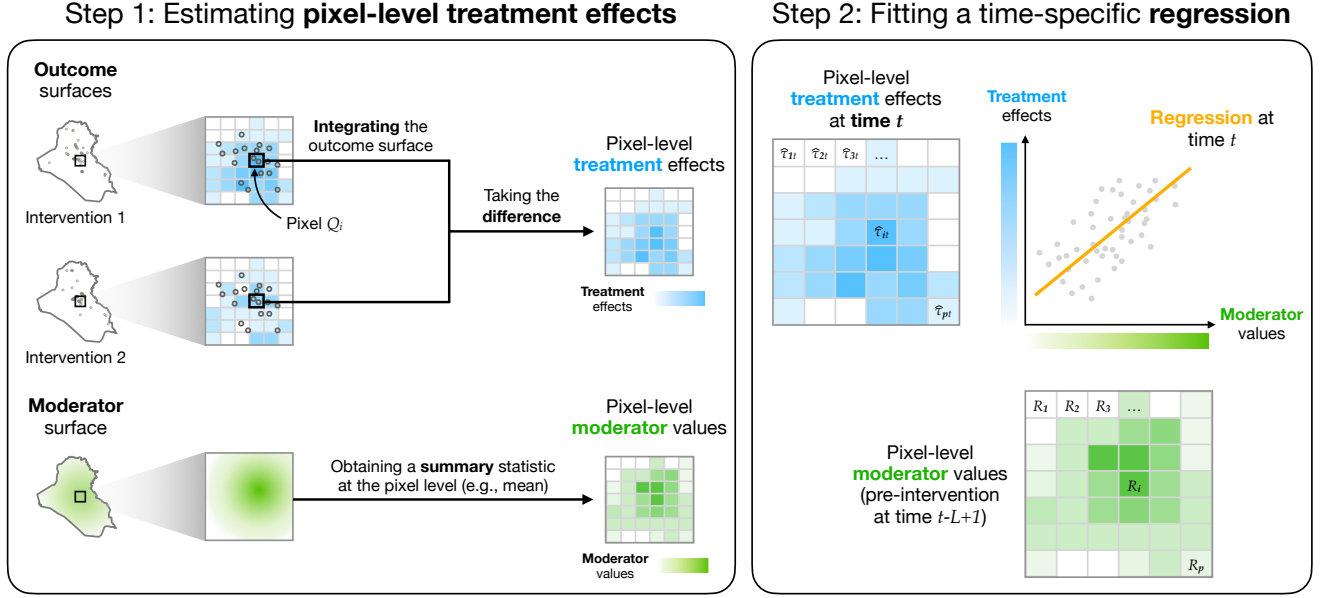


Figure 4: **Schematic representation of heterogeneous treatment effect estimation procedures.** To estimate heterogeneous treatment effects, we first estimate pixel-level treatment effects (left). We then regress pixel-level treatment effects on pixel-level moderator values to summarize the relationship between moderator values and treatment effects (right).

we apply Equations (13) and (15) to pixel Q_i and obtain a pixel-level causal effect estimate as follows,

$$\widehat{N}_{it}(F, L) = \int_{Q_i} \widehat{Y}_t(F, L; \omega) d\omega, \quad \text{and} \quad \widehat{\tau}_{it}(F', F'', L) = \widehat{N}_{it}(F'', L) - \widehat{N}_{it}(F', L).$$

We next obtain the coefficient estimates in Equation (6) by fitting a time-specific least squares regression,

$$\widehat{\beta}_t = \arg \min_{\beta_t} (\widehat{\tau}_t - \mathbf{Z}_t \beta_t)^\top (\widehat{\tau}_t - \mathbf{Z}_t \beta_t)$$

where $\widehat{\tau}_t = (\widehat{\tau}_{1t}(F', F'', L), \dots, \widehat{\tau}_{pt}(F', F'', L))^\top$ is the vector of causal effect estimators for all pixels at time t , and $\mathbf{Z}_t = [\mathbf{z}(\mathbf{R}_{1,t-L+1}), \dots, \mathbf{z}(\mathbf{R}_{p,t-L+1})]^\top$ is the matrix of p moderators across all pixels. The functional form \mathbf{z} is determined by researchers or can be made flexible, using spline basis functions.

Finally, using the estimated coefficients, we can obtain the projection CATE estimator as follows:

$$\widehat{\tau}_{F', F''}^{\text{Proj.}}(\mathbf{r}; \beta_L^*, \dots, \beta_T^*) = \mathbf{z}(\mathbf{r})^\top \left(\frac{1}{T - L + 1} \sum_{t=L}^T \widehat{\beta}_t \right). \quad (16)$$

While the estimator in Equation (16) is based on IPW, Hájek estimators can also be obtained by normalizing the weights. Zhou et al. (2024) show that this estimator is consistent and asymptotically normal.

4.3 Causal mediation analysis

We now turn to causal mediation analysis, which is the main methodological contribution of this paper. We first extend Assumptions 1 and 2 by incorporating mediators. Formally, let $F = (F_W, F_{M|w})$ be an intervention on the treatment and mediator, where f_W and $f_{M|w}$ denote the densities of F_W and $F_{M|w}$, respectively. In addition to the unconfoundedness for the treatment assignment, we also require that the realized mediator point patterns are conditionally independent of *both past and future* potential outcomes and confounders, given the observed history.

Assumption 3 (Unconfoundedness with mediators). *The treatment assignment at time t does not depend on any unobserved potential outcomes or potential values for the time-varying confounders given the observed history:*

$$f(W_t | \overline{W}_{t-1}, \overline{M}_{t-1}, \overline{Y}_T, \overline{X}_T) = f(W_t | \overline{H}_{t-1}).$$

In addition, the mediator assignment at time t does not depend on any unobserved potential values given the history including the treatment assignment:

$$f(M_t | \overline{W}_t, \overline{M}_{t-1}, \overline{Y}_T, \overline{X}_T) = f(M_t | W_t, \overline{H}_{t-1}).$$

We should note that Assumption 3 rules out the presence of (observed or unobserved) post-treatment confounders that can be affected by the contemporaneous treatment W_t and confound the mediator-outcome relationship (Imai et al., 2011; Acharya, Blackwell and Sen, 2016). In our application, this assumption is reasonable since civilian casualties occur almost instantaneously after an airstrike. The assumption may not be credible in other settings, in which much longer time passes after the treatment assignment and before the realization of mediator. Lastly, as before, we make the overlap assumption.

Assumption 4 (Bounded relative overlap with mediators). *The density ratio between the treatment and mediator point patterns of the realized data and those of the hypothetical intervention is bounded, i.e., there exist positive constants δ_W, δ_M such that*

$$f(w | \overline{H}_{t-1}) > \delta_W \cdot f_W(w) \quad \text{and} \quad f(m | \overline{H}_{t-1}, W_t = w) > \delta_M \cdot f_{M|w}(m).$$

for all $w \in \mathcal{W}$ and $m \in \mathcal{M}$.

We refer to $\rho_t(m) = f(m | \overline{H}_{t-1}, W_t)$ as the mediator score.

With the restated assumptions, we now extend general causal estimators to account for the presence of mediators. We can achieve this by incorporating the density ratio of mediators into the weights. For intervention $F = (F_W, F_{M|w})$ with corresponding densities $f_W, f_{M|w}$, define the weight of time period t according to intervention F ,

$$\xi_t(F, L) = \prod_{t'=t-L+1}^t \frac{f_W(W_{t'}) f_{M|W_{t'}}(M_{t'})}{e_{t'}(W_{t'}) \rho_{t'}(M_{t'})}.$$

Then we can define analogs of Equations (12), (13), and (14) by replacing $\zeta_t(F, L)$ by $\xi_t(F, L)$ as follows:

$$\begin{aligned}\widehat{Y}_{tm}(F, L; \omega) &= \xi_t(F, L) \widetilde{Y}_t(\omega), \quad \widehat{\mathbf{N}}_{Btm}(F, L) = \int_B \widehat{Y}_{tm}(F, L; \omega) d\omega, \\ \widehat{\mathbf{N}}_{Bm}(F, L) &= \frac{1}{T - L + 1} \sum_{t=L}^T \widehat{\mathbf{N}}_{Btm}(F, L).\end{aligned}$$

Finally, the estimators of the total, direct, and indirect effects of a fixed region B are defined as

$$\begin{aligned}\widehat{\tau}_{Bm}(F', F'', L) &= \widehat{\mathbf{N}}_{Bm}(F'', L) - \widehat{\mathbf{N}}_{Bm}(F', L), \\ \widehat{\tau}_{Bm}^{\text{DE}}(F'_W, F''_W; L, F_{M|w}) &= \widehat{\tau}_{Bm}((F'_W, F_{M|w}), (F''_W, F_{M|w}), L), \\ \widehat{\tau}_{Bm}^{\text{IE}}(F'_{M|w}, F''_{M|w}; L, F_W) &= \widehat{\tau}_{Bm}((F_W, F'_{M|w}), (F_W, F''_{M|w}), L).\end{aligned}$$

While these estimators are based on IPW, we employ Hájek estimators by normalizing weights, which we find to be much more stable in practice. In Appendix B, we show that the estimators are consistent and asymptotically normal.

5 Empirical analysis of airstrikes and insurgent attacks in Iraq

To illustrate our generalized spatiotemporal causal inference method, we examine three key debates regarding the causal relationships between airstrikes and insurgent attacks in Iraq: the *overall effects* of airstrikes on insurgent attacks (e.g., Pape, 1996; Lyall, 2014; Condra and Shapiro, 2012), the *effect heterogeneity* based on troop characteristics as a moderator (Lyall, 2014), and *causal mechanisms* through civilian casualties (e.g., Condra and Shapiro, 2012; Lyall, 2014; Dell and Querubin, 2018). For each of the three analyses, we present our hypotheses, estimation procedures, and empirical results.

Our analysis yields three main findings. First, increased airstrikes lead to heightened insurgent activities instead of their reduction. Second, airstrikes have the most pronounced effects in areas with mechanized troops, but only after at least seven days of intensified bombardment. Third, contrary to conventional wisdom, civilian casualties do not mediate the effects of airstrikes on insurgent activities. Taken together, these results suggest that insurgents meticulously plan attacks against visible targets after airstrikes.

5.1 Average treatment effects

Hypotheses. We examine the *overall effects* of airstrikes on insurgent activities from two perspectives: intensity and targeting. In the literature, the effectiveness of airstrikes during counterinsurgency operations remains unclear. In theory, targeted airstrikes that attrit and decapitate insurgents can reduce insurgent activities (Lyall, 2014; Pape, 1996). However, grievances and reputational concerns—particularly

following intensified airstrikes—may instead motivate insurgents to escalate their activities (Condra and Shapiro, 2012; Kalyvas, 2006; Carr, 2003). These arguments highlight the importance of assessing whether the intensity and targeting of airstrikes influence the dynamics of insurgent activity.

We therefore test two hypotheses related to the effectiveness of airstrikes. First, we examine whether the *intensification* of airstrikes leads to increased insurgent activity. If grievances and reputational concerns drive insurgents, then more intense airstrikes should result in heightened insurgent responses. To evaluate the effects of intensified airpower, we design a counterfactual intervention in which we increase the average number of daily airstrikes from one to 2–6, while maintaining their spatial distribution. The choice of 1-6 daily airstrikes reflects the actual number of airstrikes in our in-sample data.

Second, we test whether the *targeting* of airstrikes leads to reduced insurgent activities. We design another counterfactual intervention, in which we concentrate airstrikes to roads in Baghdad while keeping their intensity constant. This counterfactual intervention examines the effects of more targeted airstrikes on insurgent groups because roads in Baghdad are common locations for insurgent vehicles.

Estimation procedures. Our estimation procedures of the ATE involve two key steps: estimation of propensity scores and estimation of causal effects. Estimating propensity scores requires modeling the spatiotemporal distribution of airstrikes. Once propensity scores are estimated, we design counterfactual stochastic interventions and estimate causal effects.

We estimate propensity scores by modeling the locations of airstrikes as an inhomogeneous Poisson process. The locations of airstrikes are influenced by their demographic and political characteristics, distances from strategic targets, and histories of airstrikes and insurgent activities. We therefore adjust for the amount of aid and population count at the district level; distances from rivers, major roads, cities, and settlements; and 1-day, 7-day, and 30-day histories of airstrikes, shows of force, and insurgent activities. Additionally, we include time splines and an indicator for the troop surge (March 25, 2007, to January 1, 2008). We examine the model performance by checking the out-of-sample prediction performance and confirm that our model captures the time trend of airstrikes (see Appendix Figure S1).

To design a counterfactual intervention for our intensification hypothesis, we adjust the normalized airstrike density from 2006 (hereafter, “baseline density”) by multiplying it by the target daily airstrike count. Since the baseline density is normalized to integrate to one, this multiplication yields the desired counterfactual scenarios. As shown in Figure 5a, this approach increases airstrike density while preserving spatial distribution.

For our targeting hypothesis, we leverage granular geospatial data of major road objects in Iraq as well as a distance map to Baghdad to design a counterfactual intervention. To design a counterfactual intervention that involves location shifts, we create a density called a power density, which is formally

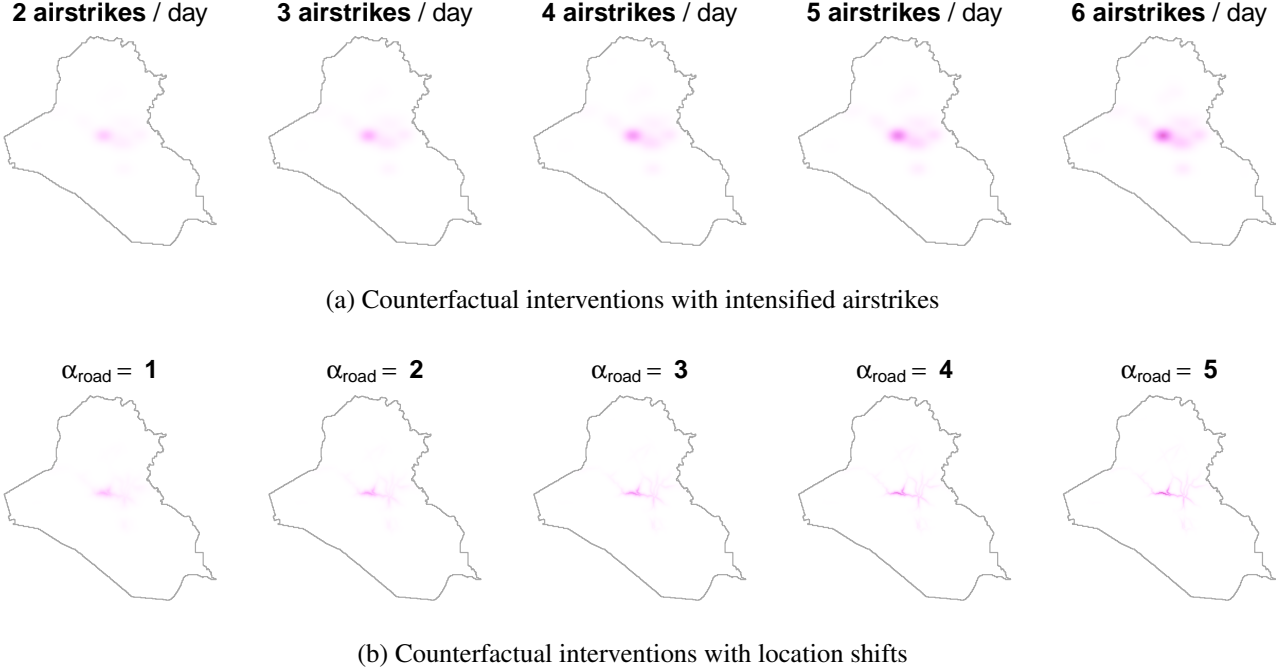


Figure 5: **Counterfactual interventions.** In Panels 5a and 5b, dark red indicates areas with high airstrike densities. Panel 5a shows counterfactual interventions with intensified airstrikes of 2–6 daily airstrikes. Panel 5b shows counterfactual interventions with location shifts. For the location-shift interventions, the average daily airstrikes is set to be five, while changing the prioritization of roads (α_{road}) over Baghdad.

defined as,

$$d_{\alpha}(\omega) = \frac{\prod_{i=1}^k d_i(\omega)^{\alpha_i}}{\int_{\Omega} \prod_{i=1}^k d_i(\omega)^{\alpha_i}},$$

where $d_i(\omega)$ denotes distributions of spatial objects of interest and α_i represents their precision parameters. In our application, we let $k = 2$ and use the distance from Baghdad ($d_1(\omega)$) and the distance from roads ($d_2(\omega)$) to construct a power density across a range of their precision parameter values. Intuitively, this approach considers several scenarios with different levels of precision applied to roads in Baghdad City. The counterfactual density is then defined as the product of the baseline density and the power density (Papadogeorgou et al., 2022; Mukaigawara et al., 2024). As shown in Figure 5b, this intervention concentrates on roads in Baghdad as road prioritization increases (by raising the value of α_{road} while maintaining $\alpha_{\text{Baghdad}} = 1$ throughout).

Results. We find that increasing the number of airstrikes from one to 2–6 per day for 7–10 days has positive effects on the number of insurgent activities (SAFs). Figure 6a summarizes the point estimates along with 95% confidence intervals. Increasing the number of airstrikes for 7–10 days results in an average expected number of SAFs ranging from 7 to 18 per day. We observe statistically significant effects consistently for treatment periods of 9–10 days, except in the case of two airstrikes over 9 days. While we do not observe statistically significant effects for improvised explosive device (IED) attacks,

we find a similar pattern: point estimates increase as we intensify the frequency and duration of airstrikes.

However, shifting the locations to roads in Baghdad does not have statistically significant effects (Figure 6b). Contrary to the intensification scenarios (Figure 6a), increased targeting of roads in Baghdad (corresponding to higher values of α_{road}) does not lead to increased insurgent activity for either SAFs or IEDs. The point estimates remain weakly negative, with no substantive changes in response to higher values of α_{road} . The effects are not statistically significant even with 9–10 days of increased targeting.

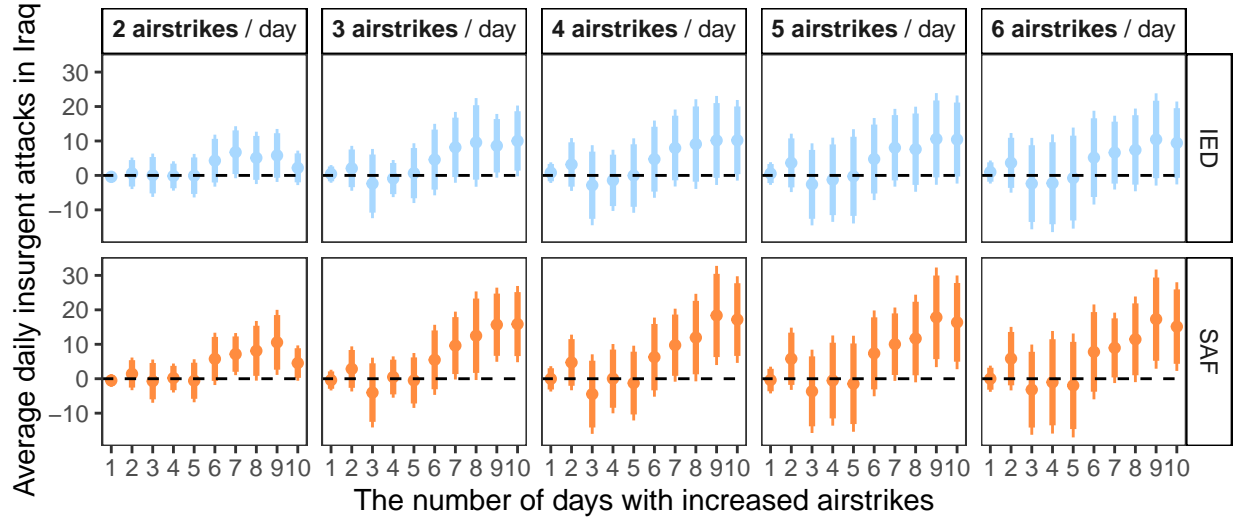
These results have three key implications. First, insurgents may take several days to respond to airstrikes, as estimated causal effects are statistically significant only after 7–10 days of counterfactual interventions. Second, the spatial distribution of insurgent activities indicates heterogeneous causal effects (see Appendix Figures S2 and S3). The analysis of heterogeneous effects shown next will shed further light on this. Third, targeting roads in Baghdad—where insurgents are often present and civilian casualties are minimal—does not yield statistically significant effects, suggesting that civilian casualties may not drive insurgent activities. Below, we conduct a mediation analysis to further investigate this possibility.

5.2 Heterogeneous treatment effects

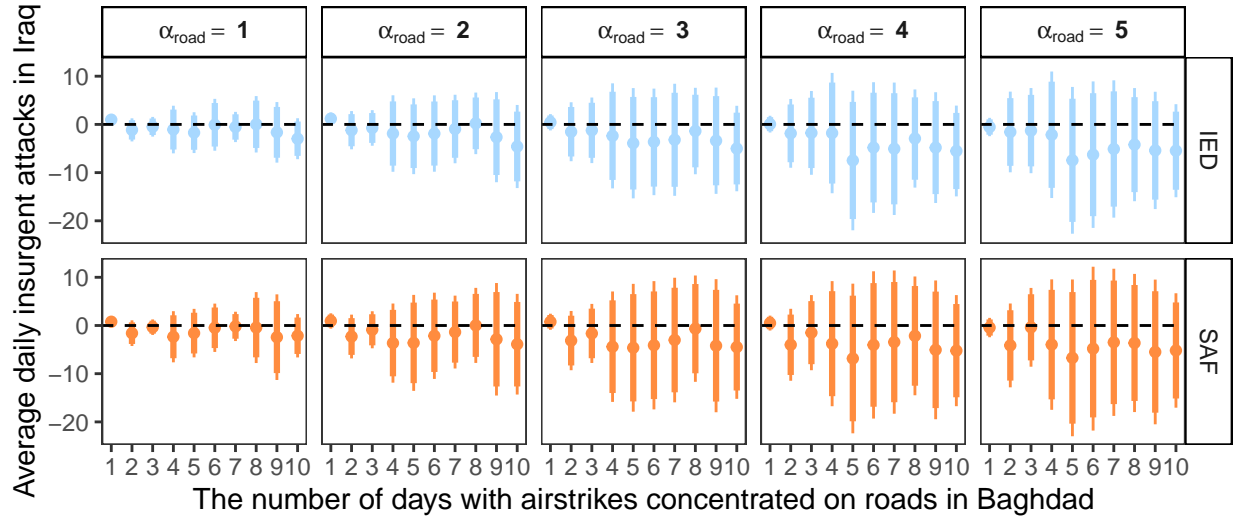
Hypotheses. An important debate concerns the *heterogeneous effects* of airstrikes on insurgent activities in relation to troop characteristics. Both grievance- and reputation-driven explanations suggest that insurgents deliberately target specific counterinsurgents. In the context of Iraq, the US Marine Corps and British Armed Forces are the most likely targets. Public opinion polls conducted by the US Department of State (Paley, 2006) and the UK Ministry of Defense (Rayment, 2005) during the Iraq War indicate strong resentment toward US and UK forces. Additionally, the US Marine Corps had a reputation for aggressive counterinsurgency tactics, including reported incidents of intentional killings of civilians (Broder, 2006). This evidence suggests that areas with a US Marine Corps or British Armed Forces presence experience intensified insurgent activity following airstrikes.

In addition to the presence of specific counterinsurgents, mechanization and troop density are crucial factors in understanding the heterogeneous effects of airstrikes on insurgent activity. Lyall and Wilson (2009) suggests that mechanized forces are often associated with increased insurgent activity because their reliance on armored vehicles limits interactions with civilians, making it harder to distinguish rebels from non-combatants. This lack of engagement can therefore heighten the risk of collateral damage, which in turn can exacerbate insurgent activities. Additionally, troop density—a key metric in counterinsurgency operations without clear empirical validation (Friedman, 2011; McGrath, 2006)—warrants further examination in the context of airstrike effectiveness. Understanding whether higher troop density deters insurgent activity is essential for planning effective counterinsurgency operations.

Our data contain four key measures of the aforementioned troop characteristics: the presence of the US Marine Corps (binary), the presence of the British Armed Forces (binary), troop mechanization



(a) Increasing the number of daily average airstrikes



(b) Focusing on roads in Baghdad

Figure 6: **Average treatment effects.** Panel 6a shows the effects of increasing the number of daily airstrikes from 1 per day to 2-6 per day without changing their spatial distributions. Panel 6b shows the effects of focusing airstrikes on roads in Baghdad, with different values of α_{road} from 1 to 5, compared to the baseline distribution of airstrikes. The number of airstrikes is set to five per day. The x-axis represents the number of days with stochastic interventions. Thick and thin lines indicate 95% and 90% confidence intervals, respectively.

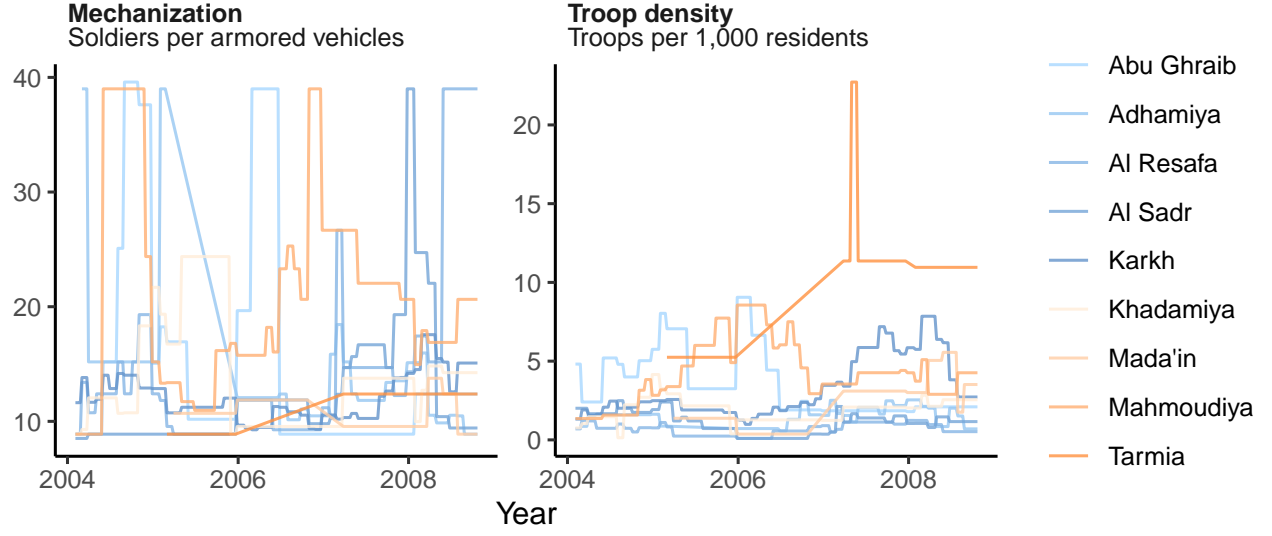


Figure 7: **Troop characteristics: Mechanization and troop density.** Each line represents one of the nine districts in the Baghdad Governorate. Even within Baghdad, both mechanization and troop density exhibit temporal and spatial variations. See SI Figures S4 and S5 for data from all districts.

(measured by the number of soldiers per armored vehicle), and troop density (measured by the number of troops per 1,000 local residents). These measures were recorded at the district-week level during the study period and exhibit both temporal and spatial variations. For example, Figure 7 illustrates the temporal trend of mechanization and troop density across nine districts within Baghdad Governorate. Even within Baghdad, we observe significant temporal and spatial variations in both mechanization and troop density.

Estimation procedures. We continue to rely on the estimated propensity score and the counterfactual intervention used for the ATE. We examine whether troop characteristics predict treatment effects when the frequency of airstrikes increases from one to 2–6 per day. For binary moderators, we consider the following linear regression model,

$$\tau_{t,F',F''}^{\text{Proj.}}(\mathbf{r}; \boldsymbol{\beta}_t^*) = \beta_{t,0} + \beta_{t,1}r,$$

and for continuous moderators, we employ:

$$\tau_{t,F',F''}^{\text{Proj.}}(\mathbf{r}; \boldsymbol{\beta}_t^*) = \sum_{l=0}^5 \beta_{t,l} z_l(r),$$

where z_l is a natural cubic spline basis of troop mechanization and troop density.

Results. We find that mechanization plays a significant role, while other troop characteristics do not (Figures 8 and 9). For the presence of the US Marine Corps and the British Armed Forces, we identify no statistically significant difference in IED and SAF occurrences between areas with and without these forces (Figure 8). As shown in Figure 8a, while the point estimates in areas without the US Marine Corps are higher than those in areas without, we observe no significant differences between areas with and without the presence of the US Marine Corps. For the British Armed Forces (Figure 8b), the CATEs are similar across all interventions.

For continuous moderators, however, Figure 9 shows that troop mechanization predicts treatment effects. Specifically, when daily airstrikes increase from one to six over 7–10 days, areas with highly mechanized troops experience greater insurgent activities than those without (see Figure 9a). We do not see similar trends for troop density (Figure 9b).

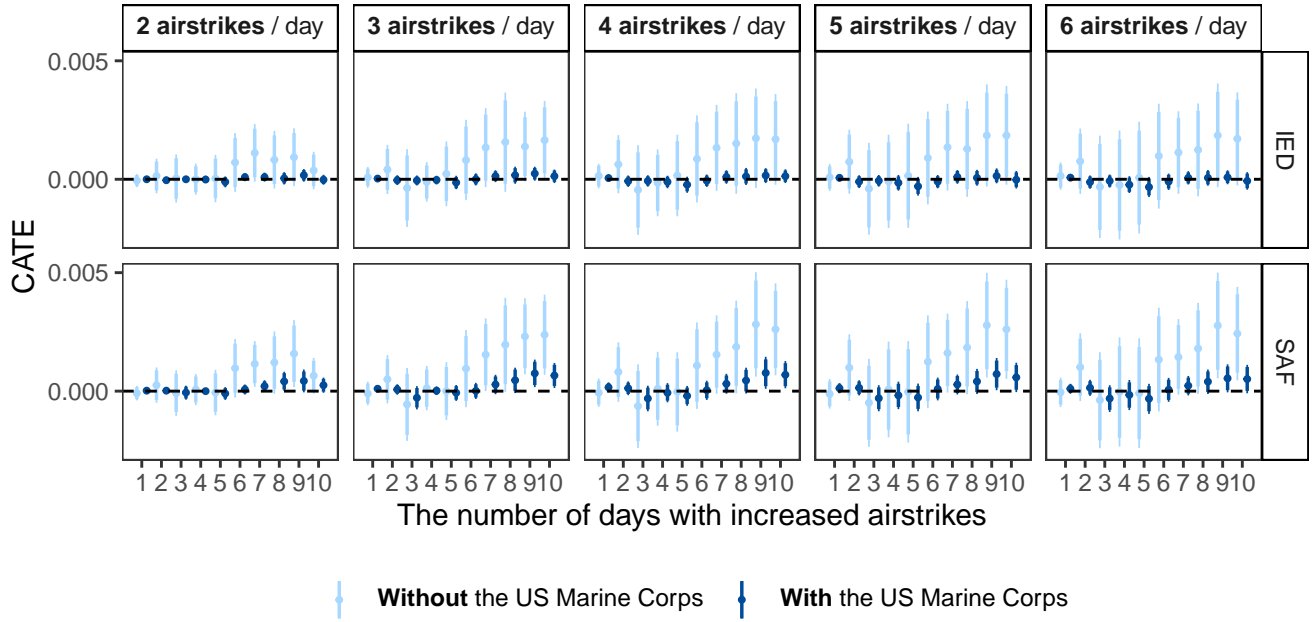
Our findings suggest that insurgents may prepare attacks on visible targets to demonstrate their resolve. We find that mechanization predicts effect heterogeneity, but only after 7–10 days of intensified airstrikes. This finding implies that insurgents need time to respond to airstrikes and selectively attack visible targets. Existing studies suggest that mechanized troops can negatively affect counterinsurgency outcomes due to limited direct interaction with local populations (Lyall and Wilson, 2009; Van Wie and Walden, 2022a; Mehrl, 2023). Our results highlight an additional factor—visibility—by which mechanized forces may influence counterinsurgency outcomes.

Additionally, contrary to the conventional use of troop density as a key indicator during counterinsurgency operations (Friedman, 2011; McGrath, 2006), we find little evidence that troop density moderates the effects of airstrikes on insurgent activity. This is in keeping with several existing studies that question the use of troop density as a key metric because it lacks an empirical basis and relies on conventional rules of thumb (Friedman, 2011; McGrath, 2006).

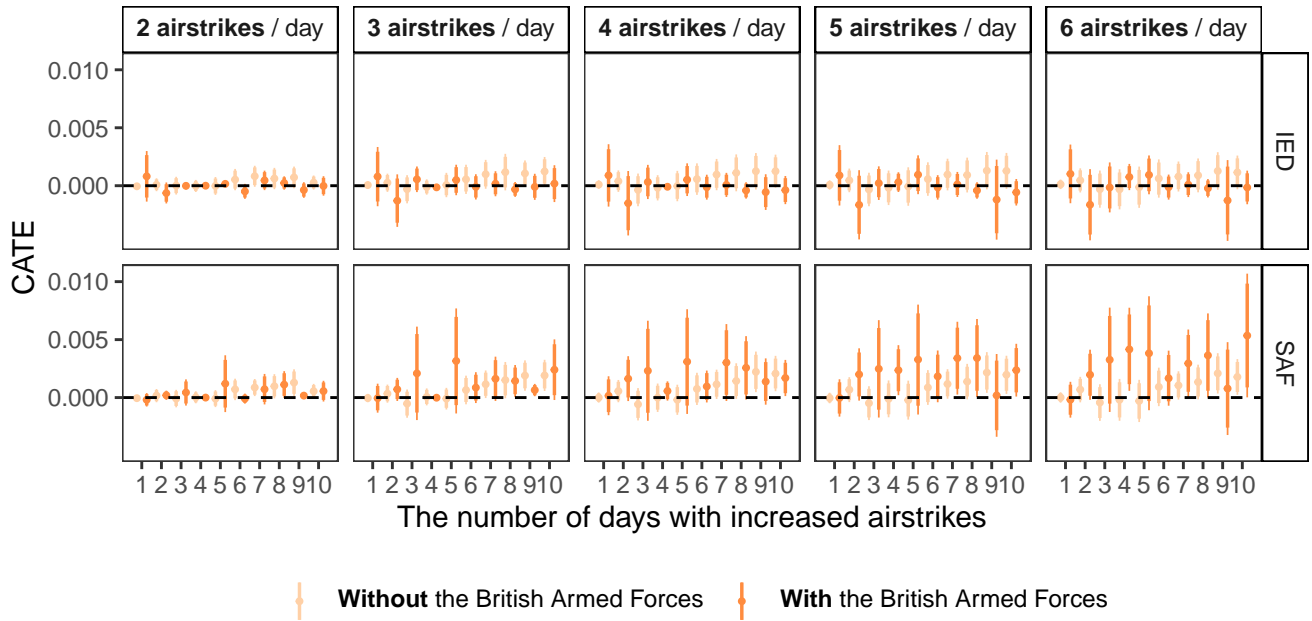
Finally, our results suggest that grievance-based explanations may not hold in Iraq. If insurgent activity were motivated by grievances, areas with troops of particular origins would experience more attacks. Yet, this does not appear to be the case, since the presence of the US Marine Corps or British Armed Forces does not moderate the causal effects. To further examine the role of grievances, we next turn to a causal mediation analysis focusing on civilian casualties as a mediator.

5.3 Causal mediation analysis

Hypotheses. Scholars have paid close attention to the causal *mechanism* question of how airstrikes affect insurgent activities through civilian casualties (e.g., Condra and Shapiro, 2012; Condra et al., 2010; Kocher, Pepinsky and Kalyvas, 2011; Johnston and Sarbahi, 2016; Dell and Querubin, 2018; Lyall, 2014; Krick, Petkun and Revkin, 2023; Thier and Ranjbar, 2008), yet no definitive conclusion has been drawn so far. Theoretically, civilian casualties can deter non-combatants to join rebellion and thus weaken insurgents. Yet they can also foster grievances and potentially increase support for insurgents.

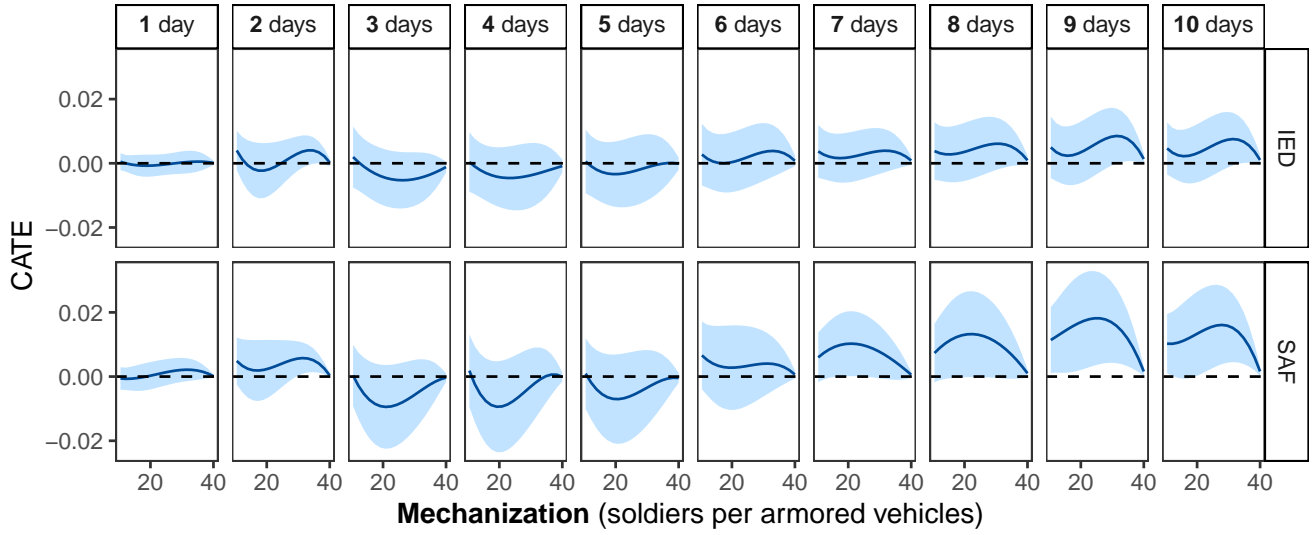


(a) US Marine Corps

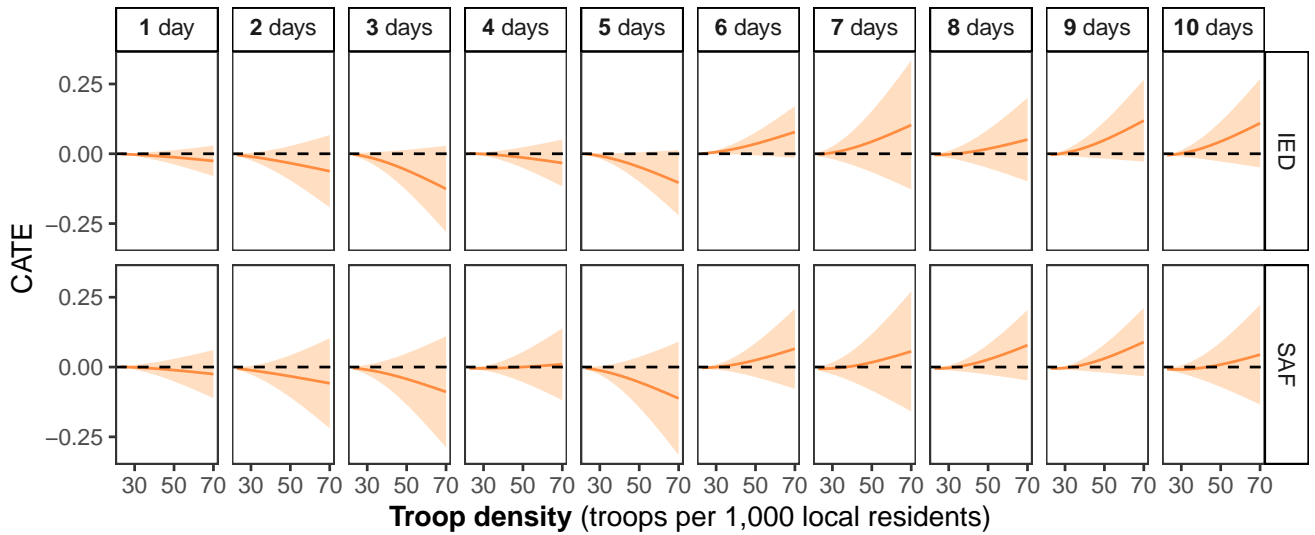


(b) British Armed Forces

Figure 8: **Heterogeneous treatment effects (the presence of the US Marine Corps and the British Armed Forces).** Heterogeneous treatment effects with respect to the presence of the US Marine Corps (Panel 8a) and the British Armed Forces (Panel 8b). Dark and light colors indicate the average treatment effects in areas with and without these troops, respectively. Thick and thin lines indicate 95% and 90% confidence intervals, respectively. The results imply that the presence of the US Marine Corps and the British Armed Forces does not affect the effects of airstrikes on insurgent activities (both IED and SAF) in Iraq.



(a) Mechanization



(b) Troop density

Figure 9: **Heterogeneous treatment effects (mechanization and the density of troops)**. Heterogeneous treatment effects with respect to mechanization (Panel 9a) and the density of troops (Panel 9b). Lines indicate point estimates. Shaded areas indicate 95% confidence intervals of CATE. The x-axis represents the number of days with stochastic interventions. We examine whether increasing daily airstrikes from one to six per day results in heterogeneous treatment effects. Mechanization (Panel 9a) is associated with intensified insurgent activities (both IED and SAF) in response to seven or more days of intensified airstrikes.

Since airstrikes almost always involve collateral damages, the effects of civilian casualties are of both theoretical and practical importance.

Examining the mediating effects of civilian casualties is particularly relevant in the context of Iraq, a country marked by the presence of state-wide insurgents as well as pronounced and dynamic shifts in sectarian divisions during the war. Given the widespread presence of insurgents across Iraq, if civilian casualties foster grievances, their effects should have spillover effects across the country and thus be particularly pronounced. Additionally, with the dynamic shifts in sectarian divisions in major cities during the war (see <https://gulf2000.columbia.edu/maps.shtml>) collateral damage to civilians can have the potential to shape conflict dynamics.

To examine whether civilian casualties mediate the causal relationship between airstrikes and insurgent activities, we estimate the *indirect* effects by modifying the intensity of civilian casualties while keeping the number of airstrikes constant (see Equation (9)). Specifically, we examine whether an increase in civilian casualties from airstrikes in Baghdad City mediates the causal effects across Iraq. We focus on Baghdad City because it experienced drastic shifts in sectarian divisions between 2006 and 2008.⁴

Estimation procedures. The estimation procedures involve four key steps: estimating propensity scores, designing counterfactual stochastic interventions for airstrikes, estimating mediator scores, and designing counterfactual stochastic interventions for civilian casualties given airstrikes. Similar to propensity scores, mediator score estimation is equivalent to modeling the conditional distribution of civilian casualties.

We use the propensity scores estimated for the ATE. To design a stochastic intervention of airstrikes, we maintain the average daily number of airstrikes but concentrate them in Baghdad. This adjustment addresses the low frequency of airstrikes in Baghdad in the 2006 out-of-sample data used to generate the baseline density (0.02 average daily airstrikes), which limits meaningful analysis of the mediation effect of civilian casualties. We set the expected number of airstrikes across Iraq to six per day but concentrate them around Baghdad. This procedure adjusts the daily expected number of airstrikes in the city to four. We confirm that this level of airstrikes was actually observed in Baghdad City in the 2007 in-sample data.

We estimate mediator scores by adopting a two-stage approach. In the first stage, we model the conditional distribution of airstrikes hitting targets *other than* civilians or military targets given airstrikes. In the second stage, conditional on the results of the first stage, we model the distribution of airstrikes hitting military targets. Since civilian casualties are expected to be higher in densely populated areas and

⁴It should also be noted that in Baghdad the positions of buildings and roads remained stable after the war. Since our distance maps are based on data from after 2008, it is essential to use locations where buildings and roads were not altered during the conflict. This contrasts with Mosul where the extensive destruction made the city inappropriate for our case study.

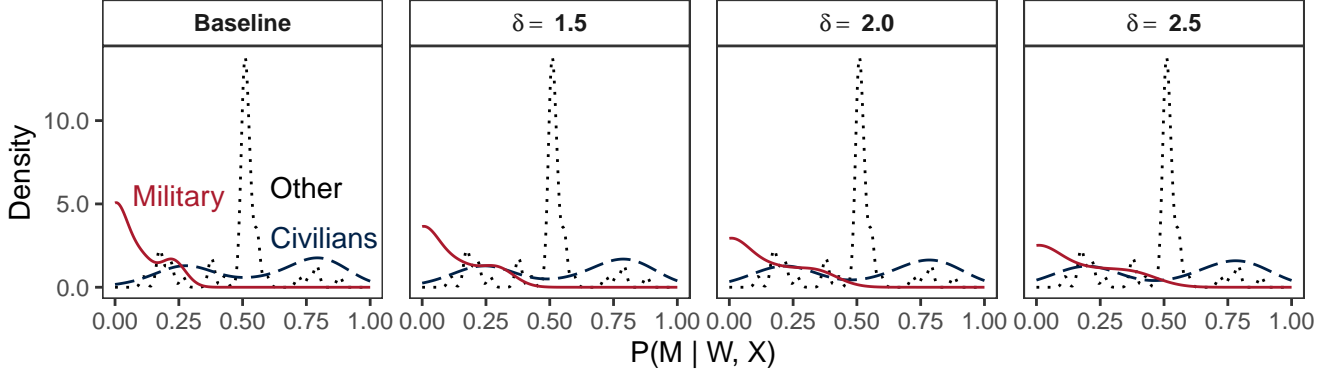


Figure 10: **Counterfactual conditional mediator densities.** The plot shows changes in the densities of conditional mediator probabilities in response to various values of δ . The conditional probabilities of hitting military targets, civilians, and other targets, given airstrike locations and covariates, are shown in red, blue, and black, respectively.

near strategic targets, we consider population density along with distance from roads, cities, residential and other buildings, and settlements as key covariates. We then employ a generalized additive model to estimate mediator scores. We evaluate the model fit using accuracy based on the area under the receiver operating characteristic curve (ROC). The area under the curve (AUC) for the first stage is 0.796, and the AUCs for the second stage are 0.781 (civilians) and 0.851 (military targets) (see Figure S6).

To design a counterfactual distribution of the mediator, we employ the incremental propensity score intervention approach proposed by Kennedy (2019). The incremental propensity score intervention allows us to avoid positivity assumptions and directly modify the conditional mediator probability with a single increment parameter $\delta \in (0, \infty)$ (Kennedy, 2019). Specifically, this approach replaces the mediator score $\Pr(M_t = m_t | W_t, \mathbf{X}_t)$ in the second stage with:

$$\Pr_{\text{new}}(M_t = m_t | W_t, \mathbf{X}_t) = \frac{\delta \Pr(M_t = m_t | W_t, \mathbf{X}_t)}{\delta \Pr(M_t = m_t | W_t, \mathbf{X}_t) + 1 - \Pr(M_t = m_t | W_t, \mathbf{X}_t)}. \quad (17)$$

where $\Pr(M_t = m_t | W_t, \mathbf{X}_t)$ represents the probability of hitting civilians (or military targets) given covariates and airstrike locations. With the incremental propensity score intervention approach, this probability is updated by the parameter $\delta > 0$, with a higher value of δ resulting in a greater updated probability $\Pr_{\text{new}}(M_t = m_t | W_t, \mathbf{X}_t)$. For example, if $\delta = 0$, then $\Pr_{\text{new}}(M_t = m_t | W_t, \mathbf{X}_t)$ equals 0, and as δ tends to infinity, the updated probability tends to 1.

We construct counterfactual conditional distributions of civilian casualties given airstrikes by setting $\delta \in \{1.5, 2, 2.5\}$. Figure 10 summarizes the changes in the densities of conditional probabilities in response to δ . The density of the conditional probability of hitting other targets (black) remains unchanged. As δ increases, the density for military targets (red) shifts right, while the density for civilians (blue) shifts left.

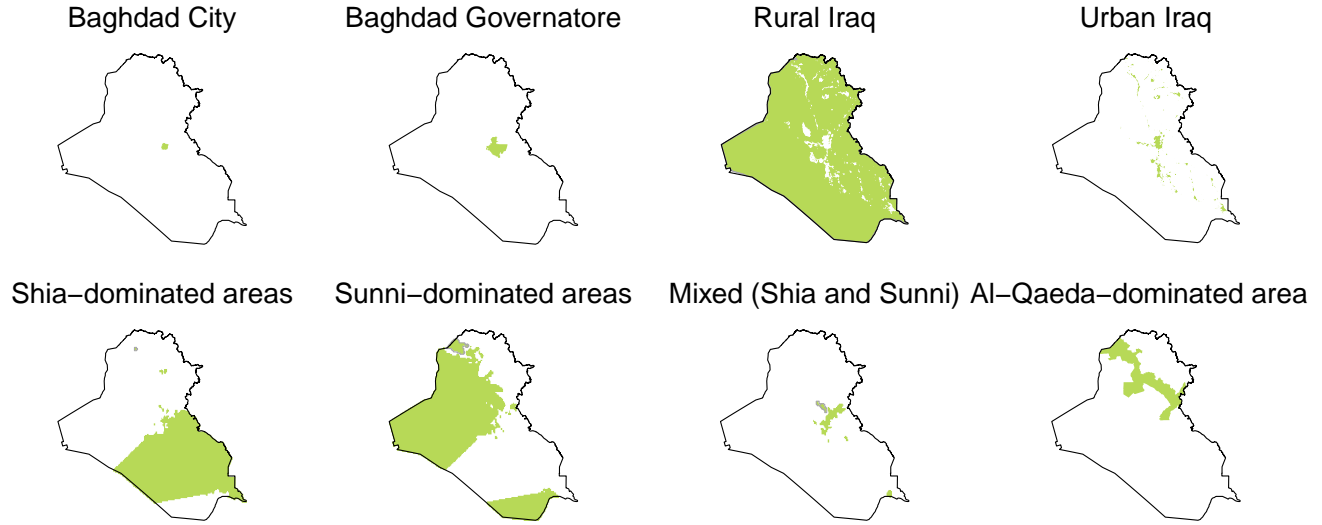


Figure 11: **Summary of key geographical areas.** Rural and urban areas are defined as areas with population count $< 300 / \text{km}^2$ and $\geq 300 / \text{km}^2$, respectively. The dominance of Sunni and Shia is determined based on [Izady \(2020\)](#). The dominance of Al-Qaeda is determined based on a map created by Coalition Forces ([Hamilton, 2008](#)). Rural Baghdad is determined as areas within Baghdad Governorate that is outside of Baghdad City.

Results. We find little evidence that altering the probability of civilian casualties in Baghdad City over one to ten days affects the number of insurgent attacks in Iraq. As summarized in Figure 12, civilian casualties have no statistically significant impact on insurgent activities, regardless of the values of δ (see Equation (17)) and L in Baghdad (see panel (a)). Given the presence of state-wide rebels in Iraq, we also test whether civilian casualties mediate the effects of airstrikes on insurgent activities in other geographically and politically salient areas (Figure 11), since grievances can, theoretically, induce indirect effects in other areas if there exist rebels that operate throughout Iraq. However, we do not find statistically significant indirect effects in any of these areas.⁵ These results suggest that civilian casualties may not mediate the relationship between airstrikes and insurgent activity.

Taken together, our spatiotemporal causal inference method reveals three key findings. First, intensifying airstrikes increases insurgent activity. Second, our analysis of heterogeneous treatment effects indicates that the causal effects align best with a resolve-based theory, in which insurgents deliberately plan attacks on visible, mechanized targets to demonstrate their resolve. This result is consistent with existing literature on mechanization in counterinsurgency ([Lyall and Wilson, 2009](#); [Van Wie and Walden, 2022a](#); [Mehrl, 2023](#)). Finally, contrary to conventional wisdom, our analysis shows that civilian casualties may not mediate the causal effects, making a grievance-based explanation less plausible in the Iraqi context.

⁵In Appendix Section E.2, we provide additional analyses focusing on other areas. Moreover, using a binary civilian casualty variable does not change the results (see Appendix Section E.3)

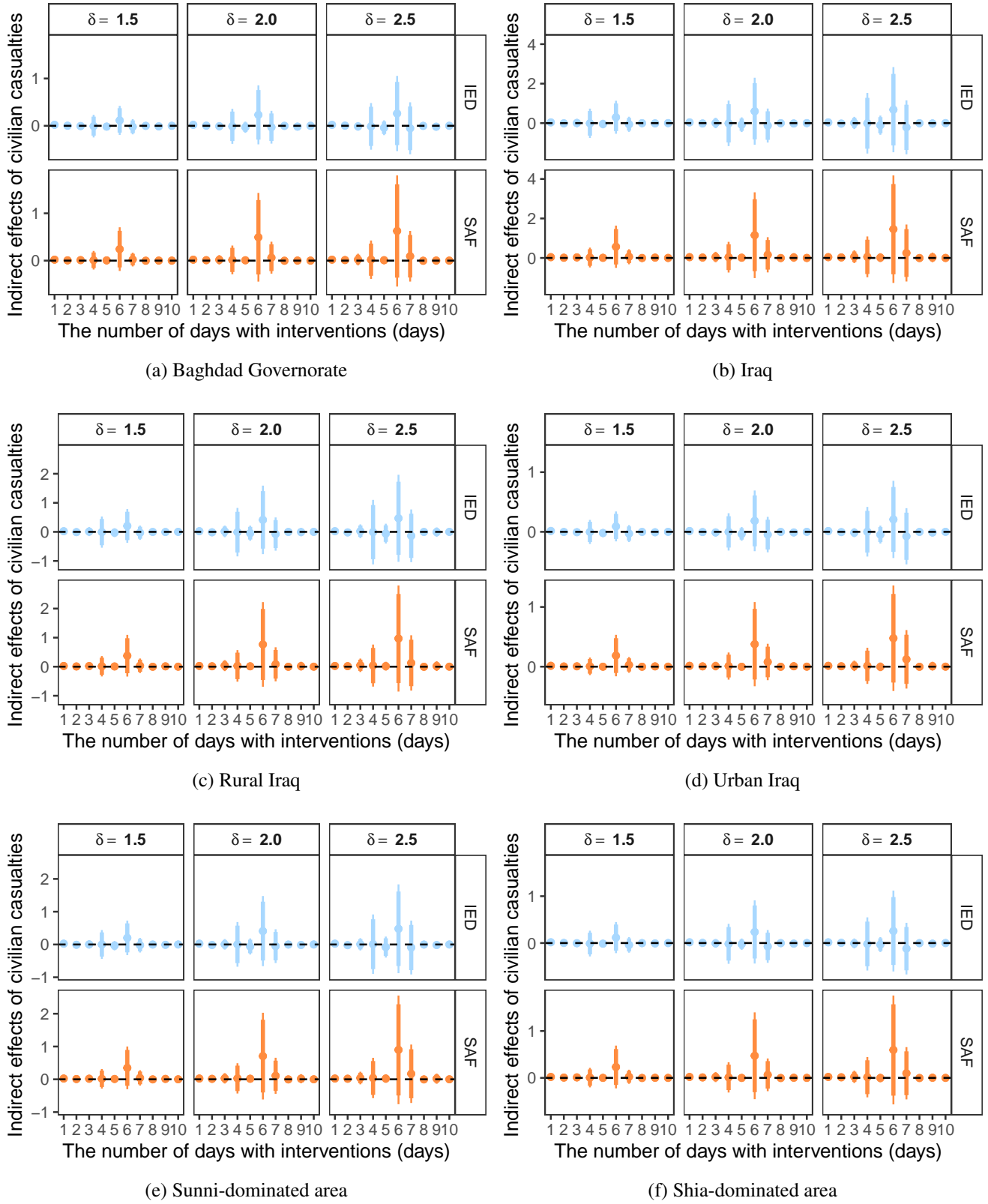


Figure 12: **Indirect effects of civilian casualties.** The dots represent the point estimates and the thick and thin bars represent the 90% and 95% confidence intervals, respectively. The x-axis represents the number of days with stochastic interventions.

6 Concluding Remarks

Despite the abundance of micro-level data, methods to fully leverage such data remain underdeveloped. To address this gap, we have developed and demonstrated a general framework for spatiotemporal causal inference that directly handles micro-level data. The proposed methodology enables the estimation of the ATE, heterogeneous treatment effects, and causal mediation analyses under a unified framework that preserves the granularity of micro-level, spatiotemporal data. Our methods are implemented through an open-source software package so that applied researchers can use them in their own analyses.

We illustrate our methodology by investigating the effects of airstrikes on insurgent activities in Iraq by estimating average treatment effects, analyzing heterogeneous treatment effects, and performing causal mediation analysis. Our findings suggest that airstrikes lead to intensified insurgent activities. However, contrary to the conventional wisdom, the effects are not mediated by civilian casualties. Instead, insurgents appear to attack mechanized, visible targets, presumably to demonstrate their resolve.

Micro-level data are becoming increasingly common in political and other social science disciplines. Our methodology could help researchers answer theoretically important and practically relevant questions in an unusually granular way. Additionally, as these data also come from fields outside political science, such as climatology and epidemiology, our methodology could help expand the scope of social science research, addressing pressing scientific questions that cross disciplinary boundaries.

References

- Abadie, Alberto. 2021. "Using Synthetic Controls: Feasibility, Data Requirements, and Methodological Aspects." *Journal of Economic Literature* 59(2):391–425.
- Acharya, Avidit, Matthew Blackwell and Maya Sen. 2016. "Explaining Causal Findings Without Bias: Detecting and Assessing Direct Effects." *American Political Science Review* 110(3):512–529.
- Aiken, Emily, Suzanne Bellue, Dean Karlan, Chris Udry and Joshua E. Blumenstock. 2022. "Machine learning and phone data can improve targeting of humanitarian aid." *Nature* 603(7903):864–870.
- Alkhuzai, Amir H., Ihsan J. Ahmad, Mohammed J. Hweel, Thakir W. Ismail, Hanan H. Hasan, Abdul Rahman Younis, Osman Shawani, Vian M. Al-Jaf, Mahdi M. Al-Alak, Louay H. Rasheed, Suham M. Hamid, Naeema Al-Gasseer, Fazia A. Majeed, Naira A. Al Awqati, Mohamed M. Ali, J. Ties Boerma and Colin Mathers. 2008. "Violence-Related Mortality in Iraq from 2002 to 2006." *New England Journal of Medicine* 358(5):484–493.
- Andrews, Ryan M. and Vanessa Didelez. 2021. "Insights into the Cross-world Independence Assumption of Causal Mediation Analysis." *Epidemiology (Cambridge, Mass.)* 32(2):209–219.
- Baddeley, Adrian. 2015. *Spatial point patterns : methodology and applications with R*. Interdisciplinary statistics first edition. ed. Boca Raton, FL: Chapman and Hall/CRC, an imprint of Taylor and Francis.
- Bautista, Maria Angélica, Felipe González, Luis R. Martínez, Pablo Muñoz and Mounu Prem. 2023. "The Geography of Repression and Opposition to Autocracy." *American Journal of Political Science* 67(1):101–118.
- Benmelech, Efraim, Claude Berrebi and Esteban F. Klor. 2015. "Counter-Suicide-Terrorism: Evidence from House Demolitions." *Journal of Politics* 77(1):27–43.
- Biddle, Stephen, Jeffrey A. Friedman and Jacob N. Shapiro. 2012. "Testing the Surge: Why Did Violence Decline in Iraq in 2007?" *International Security* 37(1):7–40.
- Blair, Christopher W. 2024. "The Fortification Dilemma: Border Control and Rebel Violence." *American Journal of Political Science* 68(4):1366–1385.
- Bojinov, Iavor and Neil Shephard. 2019. "Time Series Experiments and Causal Estimands: Exact Randomization Tests and Trading." *Journal of the American Statistical Association* 114(528):1665–1682.
- Broder, John M. 2006. "Contradictions Cloud Inquiry Into 24 Iraqi Deaths." *The New York Times* .

- Cansunar, Asli. 2022. "Distributional Consequences of Philanthropic Contributions to Public Goods: Self-Serving Elite in Ottoman Istanbul." *Journal of Politics* 84(2):889–907.
- Carr, Caleb. 2003. *The Lessons of Terror : A History of Warfare Against Civilians*. Rev. and updated, random house trade pbk. ed. ed. New York: Random House Trade Paperbacks.
- Cho, Wendy K. Tam and James G. Gimpel. 2010. "Rough Terrain: Spatial Variation in Campaign Contributing and Volunteerism." *American Journal of Political Science* 54(1):74–89.
- Christensen, Darin. 2019. "Concession Stands: How Mining Investments Incite Protest in Africa." *International Organization* 73(1):65–101.
- Condra, Luke N. and Jacob N. Shapiro. 2012. "Who Takes the Blame? The Strategic Effects of Collateral Damage." *American Journal of Political Science* 56(1):167–187.
- Condra, Luke N, Joseph H Felter, Radha K Iyengar and Jacob N Shapiro. 2010. "The Effect of Civilian Casualties in Afghanistan and Iraq." *NBER Working Paper Series* p. 16152.
- Cox, Christian, Derek A. Epp and Michael E. Shepherd. 2024. "Access to Healthcare and Voting: The Case of Hospital Closures in Rural America." *American Political Science Review* pp. 1–12.
- Crosson, Jesse and Jaclyn Kaslofsky. 2024. "Do Local Roots Impact Washington Behaviors? District Connections and Representation in the US Congress." *American Political Science Review* pp. 1–18.
- Csörgö, Miklós. 1968. "On the Strong Law of Large Numbers and the Central Limit Theorem for Martingales." *Transactions of the American Mathematical Society* 131(1):259–275.
- Davies, Shawn, Garoun Engström, Therése Pettersson and Magnus Öberg. 2024. "Organized violence 1989–2023, and the prevalence of organized crime groups." *Journal of Peace Research* 61(4):673–693.
- Dell, Melissa and Pablo Querubin. 2018. "Nation Building Through Foreign Intervention: Evidence from Discontinuities in Military Strategies." *The Quarterly Journal of Economics* 133(2):701–764.
- Díaz, Iván and Nima S. Hejazi. 2020. "Causal mediation analysis for stochastic interventions." *Journal of the Royal Statistical Society. Series B, Statistical methodology* 82(3):661–683.
- Friedman, Jeffrey A. 2011. "Manpower and Counterinsurgency: Empirical Foundations for Theory and Doctrine." *Security studies* 20(4):556–591.
- Hamilton, Eric. 2008. Developments Fighting Al Qaeda in Iraq. In *Institute for the Study of War, Jan 2008*, 8 pp.

- Harris, J. Andrew and Daniel N. Posner. 2019. “(Under What Conditions) Do Politicians Reward Their Supporters? Evidence from Kenya’s Constituencies Development Fund.” *American Political Science Review* 113(1):123–139.
- Hızlı, Çağlar, ST John, Anne Juuti, Tuure Saarinen, Kirsi Pietiläinen and Pekka Marttinen. 2023. “Temporal Causal Mediation through a Point Process: Direct and Indirect Effects of Healthcare Interventions.”
URL: <https://arxiv.org/abs/2306.09656>
- Imai, Kosuke, In Song Kim and Erik H. Wang. 2023. “Matching Methods for Causal Inference with Time-Series Cross-Sectional Data.” *American Journal of Political Science* 67(3):587–605.
- Imai, Kosuke, Luke Keele, Dustin Tingley and Teppei Yamamoto. 2011. “Unpacking the Black Box of Causality: Learning about Causal Mechanisms from Experimental and Observational Studies.” *American Political Science Review* 105(4):765–789.
- Imai, Kosuke, Luke Keele and Teppei Yamamoto. 2010. “Identification, Inference and Sensitivity Analysis for Causal Mediation Effects.” *Statistical Science* 25(1):51–71.
- Imai, Kosuke and Marc Ratkovic. 2013. “Estimating Treatment Effect Heterogeneity in Randomized Program Evaluation.” *Annals of Applied Statistics* 7(1):443–470.
- Izady, Michael. 2020. “Gulf/2000 Project Infographs, Maps and Statistics Collection.”
URL: <https://gulf2000.columbia.edu/maps.shtml>
- Johnston, Patrick B. and Anoop K. Sarbahi. 2016. “The Impact of US Drone Strikes on Terrorism in Pakistan.” *International Studies Quarterly* 60(2):203–219.
- Kalyvas, Stathis N. 2006. *The Logic of Violence in Civil War*. Cambridge studies in comparative politics Cambridge ; New York: Cambridge University Press.
- Kennedy, Edward H. 2019. “Nonparametric Causal Effects Based on Incremental Propensity Score Interventions.” *Journal of the American Statistical Association* 114(526):645–656.
- Khan, Azmat. 2021. “Hidden Pentagon Records Reveal Patterns of Failure in Deadly Airstrikes.” *The New York Times* .
- Khan, Azmat and Anand Gopal. 2017. “The Uncounted.” *The New York Times* .
- Khan, Azmat and Ivor Prickett. 2021. “The Human Toll of America’s Air Wars.” *The New York Times* .

- Kocher, Matthew Adam, Thomas B. Pepinsky and Stathis N. Kalyvas. 2011. "Aerial Bombing and Counterinsurgency in the Vietnam War." *American Journal of Political Science* 55(2):201–218.
- Krick, Benjamin, Jonathan Petkun and Mara R Revkin. 2023. "Civilian Harm and Military Legitimacy in War." *Duke Law School Public Law & Legal Theory Series* 67.
- Künzel, Sören R., Jasjeet S. Sekhon, Peter J. Bickel and Bin Yu. 2019. "Metalearners for estimating heterogeneous treatment effects using machine learning." *Proceedings of the National Academy of Sciences* 116(10):4156–4165.
- Lin, Erin. 2022. "How War Changes Land: Soil Fertility, Unexploded Bombs, and the Underdevelopment of Cambodia." *American Journal of Political Science* 66(1):222–237.
- Lok, Judith J. 2016. "Defining and estimating causal direct and indirect effects when setting the mediator to specific values is not feasible." *Statistics in Medicine* 35(22):4008–4020.
- Lok, Judith J. and Ronald J. Bosch. 2021. "Causal Organic Indirect and Direct Effects: Closer to the Original Approach to Mediation Analysis, with a Product Method for Binary Mediators." *Epidemiology (Cambridge, Mass.)* 32(3):412–420.
- Lyall, Jason. 2014. "Bombing to Lose? Airpower, Civilian Casualties, and the Dynamics of Violence in Counterinsurgency Wars.".
URL: <https://api.semanticscholar.org/CorpusID:53442618>
- Lyall, Jason and Isaiah Wilson. 2009. "Rage Against the Machines: Explaining Outcomes in Counterinsurgency Wars." *International Organization* 63(1):67–106.
- McDowall, David. 2000. *A Modern History of the Kurds*. 2nd rev. and updated ed. ed. London ; New York: I.B. Tauris.
- McGrath, John J. 2006. *Boots on the Ground: Troop Density in Contingency Operations*.
- Mehrl, Marius. 2023. "Rage and the Machines? Force Mechanization and Violence against Civilians." *Journal of Global Security Studies* 8(1):1.
- Monogan, James E., David M. Konisky and Neal D. Woods. 2017. "Gone with the Wind: Federalism and the Strategic Location of Air Polluters." *American Journal of Political Science* 61(2):257–270.
- Mukaigawara, Mitsuru, Lingxiao Zhou, Georgia Papadogeorgou, Jason Lyall and Kosuke Imai. 2024. "geocausal: An R Package for Spatio-Temporal Causal Inference.".
URL: <https://doi.org/10.31219/osf.io/5kc6f>

- Muller-Crepon, Carl. 2024. "Building tribes: How administrative units shaped ethnic groups in Africa." *American Journal of Political Science* .
- Nguyen, Trang Quynh, Ian Schmid and Elizabeth A. Stuart. 2021. "Clarifying Causal Mediation Analysis for the Applied Researcher: Defining Effects Based on What We Want to Learn." *Psychological Methods* 26(2):255–271.
- Paley, Amit R. 2006. "Most Iraqis Favor Immediate U.S. Pullout, Polls Show: Leaders' Views Out of Step With Public." *The Washington Post* p. DCA22.
- Papadogeorgou, Georgia, Kosuke Imai, Jason Lyall and Fan Li. 2022. "Causal inference with spatio-temporal data: Estimating the effects of airstrikes on insurgent violence in Iraq." *Journal of the Royal Statistical Society. Series B, Statistical methodology* 84(5):1969–1999.
- Pape, Robert Anthony. 1996. *Bombing to Win : Air Power and Coercion in War*. Cornell studies in security affairs Ithaca: Cornell University Press.
- Pierskalla, Jan H. and Florian M. Hollenbach. 2013. "Technology and Collective Action: The Effect of Cell Phone Coverage on Political Violence in Africa." *American Political Science Review* 107(2):207–224.
- Polo, Sara M. T. and Blair Welsh. 2024. "Violent Competition and Terrorist Restraint." *International Organization* pp. 1–30.
- Raleigh, Clionadh, Roudabeh Kishi and Andrew Linke. 2023. "Political instability patterns are obscured by conflict dataset scope conditions, sources, and coding choices." *Humanities & Social Sciences Communications* 10(1):74–17.
- Rayment, Sean. 2005. "Secret MoD poll: Iraqis support attacks on British troops." *Sunday telegraph (London, England)* .
- Robins, James M, Miguel Angel Hernan and Babette Brumback. 2000. "Marginal structural models and causal inference in epidemiology." *Epidemiology* pp. 550–560.
- Ruggeri, Andrea, Han Dorussen and Theodora-Ismene Gizelis. 2017. "Winning the Peace Locally: UN Peacekeeping and Local Conflict." *International Organization* 71(1):163–185.
- Runge, Jakob, Vladimir Petoukhov, Jonathan F. Donges, Jaroslav Hlinka, Nikola Jajcay, Martin Vejmelka, David Hartman, Norbert Marwan, Milan Paluš and Jürgen Kurths. 2015. "Identifying causal gateways and mediators in complex spatio-temporal systems." *Nature Communications* 6(1):8502–8502.

- Sexton, Renard and Christoph Zürcher. 2024. “Aid, Attitudes, and Insurgency: Evidence from Development Projects in Northern Afghanistan.” *American Journal of Political Science* 68(3):1168–1182.
- Sonin, Konstantin and Austin L. Wright. 2024. “Rebel Capacity, Intelligence Gathering, and Combat Tactics.” *American Journal of Political Science* 68(2):459–477.
- Sundberg, Ralph and Erik Melander. 2013. “Introducing the UCDP Georeferenced Event Dataset.” *Journal of Peace Research* 50(4):523–532.
- Tam Cho, Wendy K. and James G. Gimpel. 2007. “Prospecting for (Campaign) Gold.” *American Journal of Political Science* 51(2):255–268.
- Tchetgen Tchetgen, Eric J., Isabel R. Fulcher and Ilya Shpitser. 2021. “Auto-G-Computation of Causal Effects on a Network.” *Journal of the American Statistical Association* 116(534):833–844.
- Thier, J Alexander and Azita Ranjbar. 2008. “Killing Friends, Making Enemies: The Impact and Avoidance of Civilian Casualties in Afghanistan.”
URL: <https://www.usip.org/publications/2008/07/killing-friends-making-enemies-impact-and-avoidance-civilian-casualties>
- van der Vaart, Aad W. 2010. “TIME SERIES.” *VU University Amsterdam, lecture notes* .
- Van Wie, Ryan C. and Jacob A. Walden. 2022a. “Troops or Tanks? Rethinking COIN mechanization and force employment.” *Small wars & insurgencies* 33(6):1032–1058.
- Van Wie, Ryan and Jacob Walden. 2022b. “Replication Data for: “Troops or Tanks: Rethinking Mechanization in Iraq”.”
URL: <https://doi.org/10.7910/DVN/E9NX1Y>
- VanderWeele, Tyler. 2015. *Explanation in causal inference : methods for mediation and interaction*. 1st ed. ed. New York: Oxford University Press.
- Wager, Stefan and Susan Athey. 2018. “Estimation and Inference of Heterogeneous Treatment Effects using Random Forests.” *Journal of the American Statistical Association* 113(523):1228–1242.
- Wang, Ye, Cyrus Samii, Haoge Chang and Peter M. Aronow. 2020. “Design-Based Inference for Spatial Experiments under Unknown Interference.” *arXiv preprint arXiv:2010.13599* .
URL: <https://arxiv.org/abs/2010.13599>
- Wood, Reed M. 2014. “From Loss to Looting? Battlefield Costs and Rebel Incentives for Violence.” *International Organization* 68(4):979–999.

Xu, Yiqing, Anqi Zhao and Peng Ding. 2024. “Factorial Difference-in-Differences.”.

URL: <https://doi.org/10.48550/arXiv.2407.11937>

Young, Rachel and Solomon Hsiang. 2024. “Mortality caused by tropical cyclones in the United States.” *Nature* .

Zhang, Wenjia and Kexin Ning. 2023. “Spatiotemporal Heterogeneities in the Causal Effects of Mobility Intervention Policies during the COVID-19 Outbreak: A Spatially Interrupted Time-Series (SITS) Analysis.” *Annals of the American Association of Geographers* 113(5):1112–1134.

Zhou, Lingxiao, Kosuke Imai, Jason Lyall and Georgia Papadogeorgou. 2024. “Estimating Heterogeneous Treatment Effects for Spatio-Temporal Causal Inference: How Economic Assistance Moderates the Effects of Airstrikes on Insurgent Violence.”.

URL: <https://arxiv.org/abs/2412.15128>

Zhukov, Yuri M., Jason S. Byers, Marty A. Davidson and Ken Kollman. 2024. “Integrating Data Across Misaligned Spatial Units.” *Political Analysis* 32(1):17–33.

SUPPLEMENTARY INFORMATION FOR
“SPATIOTEMPORAL CAUSAL INFERENCE WITH
SPILLOVER AND CARRYOVER EFFECTS”

A	Literature review	2
B	Asymptotic properties	3
B.1	Definitions and assumptions	3
B.2	Theorem 1: Asymptotic normality of estimator over a fixed region B	4
B.3	Theorem 2: Asymptotic normality for estimator within d –neighborhood	8
C	Average treatment effects	14
C.1	Estimation of propensity scores	14
C.2	Estimation of causal effects	15
D	Heterogeneous treatment effects	16
D.1	Troop characteristics	16
E	Causal mediation analysis	18
E.1	Model fit	18
E.2	Main results in other geographical areas	19
E.3	Main results using an indicator for civilian casualties	20

A Literature review

We search for papers published in the *American Political Science Review* (APSR), *American Journal of Political Science* (AJPS), *Journal of Politics* (JoP), and *International Organization* (IO) using the following search terms: geographical OR geospatial OR spatial OR microdata.⁶ Due to the number of papers on spatial voting theory, we exclude the term *spatial* when searching the database of the *American Journal of Political Science*.

The aforementioned procedure yields 859 papers. After sifting the literature based on titles, abstracts, and full texts in this order, we identify 20 papers that employ micro-level data (Table S1).⁷ Of these, 16 papers (80%) aggregate data at certain geographical levels or convert them into an indicator variable and employ panel data analytic methods such as fixed effects and difference-in-differences. Four papers (20%) do not aggregate the data, but they do not proceed to causal identification.

Table S1: Summary of the literature published in top political science journals.

Citation	Journal	Data	Aggregation	Model
Pierskalla and Hollenbach (2013)	APSR	PV	Yes*	FE
Cox, Epp and Shepherd (2024)	APSR	Hospital closures	Yes [†]	FE
Crosson and Kaslovsky (2024)	APSR	Birthplaces	Yes [†]	FE
Condra and Shapiro (2012)	AJPS	PV	Yes [‡]	FE
Lin (2022)	AJPS	Bombings	Yes [§]	FE
Bautista et al. (2023)	AJPS	Military facilities	Yes [†]	IV
Blair (2024)	AJPS	PV	Yes	DiD
Sexton and Zürcher (2024)	AJPS	Aid projects	Yes [¶]	DiD
Sonin and Wright (2024)	AJPS	Counterinsurgencies	Yes	OLS
Muller-Crepon (2024)	AJPS	Ethnic groups	Yes ^{**}	RD
Benmelech, Berrebi and Klor (2015)	JoP	House demolitions	Yes	FE
Cansunar (2022)	JoP	Fountains	Yes ^{††}	FE
Wood (2014)	IO	PV	Yes	GLM
Ruggeri, Dorussen and Gizelis (2017)	IO	PV	Yes*	GLM
Christensen (2019)	IO	Mines & PV	Yes*	DiD
Polo and Welsh (2024)	IO	PV	Yes	FE
Harris and Posner (2019)	APSR	Development projects	No	PP
Tam Cho and Gimpel (2007)	AJPS	Fundraising	No	Kriging
Cho and Gimpel (2010)	AJPS	Fundraising	No	GWR
Monogan, Konisky and Woods (2017)	AJPS	Air polluters	No	PP

Note: DiD: difference-in-differences, FE: fixed effects, GLM: generalized linear model, GWR: geographically weighted regression, IV: instrumental variable, OLS: ordinary least squares, PP: Poisson process, PV: political violence, RD: (geographic) regression discontinuities. * Grid cell, [†] Indicator, [‡] Count per capita, [§] Field, ^{||} District, [¶] Village, ^{**} Enumeration area, ^{††} Neighborhood.

⁶The search was conducted on October 28, 2024 using the official publisher websites of these journals.

⁷We exclude papers that convert locations into distance metrics.

B Asymptotic properties

In this section, we derive the estimators' asymptotic distributions, and we show that they are consistent and asymptotically normal. We also discuss that the estimators' asymptotic variance cannot be estimated without additional assumptions and derive an alternative, conservative inferential approach.

B.1 Definitions and assumptions

Some useful definitions from the manuscript:

$$\begin{aligned}\xi_t(F, L) &= \prod_{t'=t-L+1}^t \frac{f_W(W_{t'})f_{M|W_{t'}}(M_{t'})}{e_{t'}(W_{t'})\rho_{t'}(M_{t'})} \\ \tilde{Y}_t(\omega) &= \sum_{s \in S_{Y_t}} K_b(\omega, s) \\ \hat{Y}_t(F, L; \omega) &= \xi_t(F, L)\tilde{Y}_t(\omega) \\ N(\tilde{Y}_t, B) &= \int_B \tilde{Y}_t(\omega) d\omega \\ N(Y_t, B) &= |S_{Y_t} \cap B|\end{aligned}$$

Some definitions that will be useful for the proofs:

- For $\epsilon > 0$, we use $\mathcal{N}_\epsilon(A)$ to denote the ϵ -neighborhood of a set A : $\mathcal{N}_\epsilon(A) = \{\omega \in \Omega : \text{dist}(\omega, a) < \epsilon\}$.
- We use ∂B to denote the boundary of B (its closure excluding the interior points), $\partial B = \overline{B} \setminus B^\circ$.

Assumption S.1 (Regularity conditions). *For each theoretical result, we require a subset of the following regularity conditions:*

- There exists $\delta_Y > 0$ such that $|S_{Y_t}(\overline{w}_t)| < \delta_Y$ for all $t \in \mathcal{T}$ and $\overline{w}_t \in \mathcal{W}^T$.*
- Let $\eta_t = \text{Var}\{[\xi_t(F^2, L) - \xi_t(F^1, L)]N(Y_t, B) \mid \overline{H}_{t-L}^*\}$ for $t \geq L$. Then, there exists $\eta \in \mathbb{R}^+$ such that $(T - L + 1)^{-1} \sum_{t=L}^T \eta_t \xrightarrow{p} \eta$ as $T \rightarrow \infty$.*
- There exists a neighborhood of set B 's boundary over which outcome active locations are observed during at most T^{1-Q^*} time periods, for some $Q^* \in (1/2, 1)$ and as $T \rightarrow \infty$, i.e. there exists $\delta_B > 0$ such that*

$$P\left(\sum_{t=L}^T I\left(\exists s \in S_{Y_t} \cap \mathcal{N}_{\delta_B}(\partial B)\right) > T^{1-Q^*}\right) \rightarrow 0, \text{ as } T \rightarrow \infty.$$

B.2 Theorem 1: Asymptotic normality of estimator over a fixed region B

Theorem 1 (Asymptotic normality of estimator over a fixed region B). *If Assumption 4 and the regularity conditions in the appendix hold, and the kernel bandwidth $b_T \rightarrow 0$, then*

$$\sqrt{T}(\widehat{\tau}_B(F', F'', L) - \tau_B(F', F'', L)) \xrightarrow[T \rightarrow \infty]{d} N(0, \eta).$$

Furthermore, $(T - L + 1)^{-1} \sum_{t=L}^T [\widehat{\tau}_{Bt}(F', F'', L)]^2$ is a consistent estimator of an upper bound of the asymptotic variance η .

Theorem 1 states that the estimator is asymptotically normally distributed, and allows us to estimate a bound for the estimator's variance assuming a long enough time series. Therefore, this result allows us to make inference on the effect for a change in the intervention of the treatment and mediator assignment on the outcome process over a region B . Since direct and indirect effects can be written in this form for carefully defined stochastic interventions (see (9) and (8)), Theorem 1 also implies that our estimators of the direct and indirect effect in (15) are consistent and asymptotically normal, which allows us to make inference on the causal pathways of the spatio-temporal point pattern treatment within a region B . We can similarly show that the estimator for the expected number of outcome active locations $\widehat{N}_B(F, L)$ is consistent for $N_B(F, L)$ and asymptotically normal, but the proof is omitted here for clarity.

Proof of Theorem 1. The proof of this theorem follows closely the proof of (Theorem 1 in Papadogeorgou et al., 2022). The main difference lies in the fact that the stochastic interventions take place over both the treatment and mediator assignment, and the causal assumptions and proof below have to be altered to accommodate that.

In what follows, we write K_{b_T} instead of K_b to reflect the dependence of the bandwidth parameter on the time series length T . The variables temporally precedent to the treatment assignment at time period t , W_t , is the expanded history $\overline{H}_{t-1}^* = \{\overline{W}_{t-1}, \overline{M}_{t-1}, \overline{Y}_T, \overline{X}_T\} \supset \overline{H}_{t-1}$. Since $\overline{H}_{t-1}^* \subset \overline{H}_t^*$, the expanded history is a filtration generated by the collection of potential values of confounders and outcomes, \overline{X}_T and \overline{Y}_T , and the previous treatments and mediator values, \overline{W}_{t-1} and \overline{M}_{t-1} . Let

$$\begin{aligned} e_{Bt} &= \widehat{\tau}_{Bt}(F', F'', L) - \tau_{Bt}(F', F'', L) \\ &= [\xi_t(F^2, L) - \xi_t(F^1, L)]N(\tilde{Y}_t, B) - \left\{ \mathbf{N}_{Bt}(F'', L) - \mathbf{N}_{Bt}(F', L) \right\} \\ &= \underbrace{[\xi_t(F^2, L) - \xi_t(F^1, L)]N(Y_t, B) - \left\{ \mathbf{N}_{Bt}(F'', L) - \mathbf{N}_{Bt}(F', L) \right\}}_{q_{1Bt}} - \underbrace{[\xi_t(F^2, L) - \xi_t(F^1, L)][N(\tilde{Y}_t, B) - N(Y_t, B)]}_{q_{2Bt}} \end{aligned} \quad (18)$$

We show that

1. $\sqrt{T}(\frac{1}{T-L+1} \sum_{t=L}^T q_{1Bt})$ is asymptotically normal, and
2. $\sqrt{T}(\frac{1}{T-L+1} \sum_{t=L}^T q_{2Bt})$ converges to zero in probability.

Showing asymptotic normality of q_{1Bt} : We use (van der Vaart, 2010, Theorem 4.16). Specifically, we show that

- (1) q_{1Bt} is a martingale difference series with respect to the filtration \bar{H}_{t-L}^* , and
- (2) for every $\epsilon > 0$, $(T - L + 1)^{-1} \sum_{t=L}^T E\{q_{1Bt}^2 I(|q_{1Bt}| > \epsilon\sqrt{T-L+1}) \mid \bar{H}_{t-L}^*\} \xrightarrow{p} 0$.

To prove that q_{1Bt} is a martingale difference series, we show that $E(|q_{1Bt}|) < \infty$ and $E(q_{1Bt} \mid \bar{H}_{t-L}^*) = 0$. For the first part, Assumption 4 and Assumption S.1(a) imply that:

$$\begin{aligned} |q_{1Bt}| &= |[\xi_t(F^2, L) - \xi_t(F^1, L)]N(Y_t, B) - \{\mathbf{N}_{Bt}(F'', L) - \mathbf{N}_{Bt}(F', L)\}| \\ &\leq [\xi_1(F, L) + \xi_2(F, L)]N(Y_t, B) + \mathbf{N}_{Bt}(F', L) + \mathbf{N}_{Bt}(F'', L) \\ &\leq 2\delta_Y(\delta_W^L \delta_M^L + 1), \end{aligned} \tag{19}$$

hence $E[|q_{1Bt}|] < \infty$. For the second part, it suffices to show that

$$E[\xi_t(F, L)N(Y_t, B) \mid \bar{H}_{t-L}^*] = \mathbf{N}_{Bt}(F, L),$$

where the expectation is taken with respect to treatments and mediators $(W_{t-L+1}, M_{t-L+1}, \dots, W_t, M_t)$:

$$\begin{aligned} &E[\xi_t(F, L)N(Y_t, B) \mid \bar{H}_{t-L}^*] \\ &= \int \left[\prod_{t'=t-L+1}^t \frac{f_W(w_{t'})f_{M|w_{t'}}(m_{t'})}{e_{t'}(w_{t'})\rho_{t'}(m_{t'})} \right] N_B(Y_t(W_1, M_1, \dots, W_{t-L}, M_{t-L}, w_{t-L+1}, m_{t-L+1}, \dots, w_t, m_t)) \times \\ &\quad f(w_{t-L+1} \mid \bar{H}_{t-L}^*) f(m_{t-L+1} \mid \bar{H}_{t-L}^*, W_{t-L+1}) \times \\ &\quad f(w_{t-L+2} \mid \bar{H}_{t-L}^*, W_{t-L+1}, M_{t-L+1}) \times \\ &\quad \dots \times \\ &\quad f(w_t \mid \bar{H}_{t-L}^*, W_{t-L+1}, M_{t-L+1}, \dots, W_{t-1}, M_{t-1}) f(m_t \mid \bar{H}_{t-L}^*, W_{t-L+1}, M_{t-L+1}, \dots, M_{t-1}, W_t) \\ &\quad d(w_{t-L+1}, m_{t-L+1}, \dots, w_t, m_t) \\ &= \int \left[\prod_{t'=t-L+1}^t \frac{f_W(w_{t'})f_{M|w_{t'}}(m_{t'})}{e_{t'}(w_{t'})\rho_{t'}(m_{t'})} \right] N_B(Y_t(W_1, M_1, \dots, W_{t-L}, M_{t-L}, w_{t-L+1}, m_{t-L+1}, \dots, w_t, m_t)) \times \\ &\quad f(w_{t-L+1} \mid \bar{H}_{t-L}^*) f(m_{t-L+1} \mid \bar{H}_{t-L}^*, W_{t-L+1}) f(w_{t-L+2} \mid \bar{H}_{t-L+1}^*) f(m_{t-L+2} \mid \bar{H}_{t-L+1}^*, W_{t-L+2}) \dots \end{aligned} \tag{20}$$

$$\begin{aligned}
& f(w_t \mid \overline{H}_{t-1}^*) f(m_t \mid \overline{H}_{t-1}^*, W_t) \\
& d(w_{t-L+1}, m_{t-L+1}, \dots, w_t, m_t) \quad (\text{because } \overline{H}_t^* = \overline{H}_{t-1}^* \cup \{W_t, M_t\}) \\
& = \int N_B(Y_t(W_1, M_1, \dots, W_{t-L}, M_{t-L}, w_{t-L+1}, m_{t-L+1}, \dots, w_t, m_t)) \prod_{t'=t-L+1}^t f_W(w_{t'}) f_{M|w_{t'}}(m_{t'}) \\
& \quad d(w_{t-L+1}, m_{t-L+1}, \dots, w_t, m_t) \quad (\text{By Assumption 4}) \\
& = \mathbf{N}_{Bt}(F, L).
\end{aligned}$$

This establishes the claim that q_{1Bt} is a martingale difference series with respect to filtration \overline{H}_{t-L}^* .

Next, let $\epsilon > 0$. Since q_{1Bt} is bounded by (19), choose T_0 as

$$\begin{aligned}
T_0 &= \operatorname{argmin}_{t \in \mathbb{N}^+} \{ \epsilon \sqrt{t - L + 1} > 2\delta_Y(\delta_W^L \delta_M^L + 1) \} \\
&= \operatorname{argmin}_{t \in \mathbb{N}^+} \left\{ t > L - 1 + \left[\frac{2\delta_Y(\delta_W^L \delta_M^L + 1)}{\epsilon} \right]^2 \right\} \\
&= \left\lceil L - 1 + \left[\frac{2\delta_Y(\delta_W^L \delta_M^L + 1)}{\epsilon} \right]^2 \right\rceil
\end{aligned} \tag{21}$$

Then, for $T > T_0$, $I(|q_{1Bt}| > \epsilon \sqrt{T - L + 1}) = 0$ and $E(q_{1Bt}^2 I(|q_{1Bt}| > \epsilon \sqrt{T - L + 1}) \mid \overline{H}_{t-L}^*) = 0$.

Combining the previous results to show asymptotic normality of the first error: Since q_{1Bt} has mean zero, $E(q_{1Bt}^2 \mid \overline{H}_{t-L}^*) = \operatorname{Var}(q_{1Bt} \mid \overline{H}_{t-L}^*)$, and since $\tau_{Bt}(F', F'', L)$ is fixed, $\operatorname{Var}(q_{1Bt} \mid \overline{H}_{t-L}^*) = \operatorname{Var}\{\xi_t(F^2, L) - \xi_t(F^1, L)]N(Y_t, B) \mid \overline{H}_{t-L}^*\} = \eta_t$. This gives us that

$$\frac{1}{T - L + 1} \sum_{t=L}^T E(q_{1Bt}^2 \mid \overline{H}_{t-L}^*) = \frac{1}{T - L + 1} \sum_{t=L}^T \eta_t \xrightarrow{p} \eta,$$

from Assumption S.1(b). From Theorem 4.16 of van der Vaart (2010),

$$\sqrt{T} \left(\frac{1}{T - L + 1} \sum_{t=L}^T q_{1Bt} \right) \xrightarrow{d} N(0, \eta).$$

Showing convergence to zero of q_{2Bt} : We want to show that for $T \rightarrow \infty$ and $b_T \rightarrow 0$ as $T \rightarrow \infty$,

$$\sqrt{T} \left(\frac{1}{T - L + 1} \sum_{t=L}^T q_{2Bt} \right) \xrightarrow{p} 0.$$

To do so, we note that the error q_{2Bt} is a weighted comparison of the outcome active locations within set B based on the observed data $N(Y_t, B)$ and the smoothed observed outcome surface $N(\tilde{Y}_t, B)$

$$\frac{1}{T-L+1} \sum_{t=L}^T q_{2Bt} = \frac{1}{T-L+1} \sum_{t=L}^T (\xi_t(F^2, L) - \xi_t(F^1, L)) \left[\int_B \sum_{s \in S_{Y_t}} K_{b_T}(\omega; s) d\omega - N_B(Y_t) \right].$$

Since $|\xi_t(F^2, L) - \xi_t(F^1, L)| \leq 2(\delta_W^L \delta_M^L + 1)$ from Assumption 4, and using Assumption S.1(c) the result can be acquired following the steps of the proof of Theorem 1 in [Papadogeorgou et al. \(2022\)](#), since the treatment and mediator assignment are nuisances in showing that this error converges to zero, and it is only required that they lead to bounded weights $\xi_t(F, L)$.

Estimator of the upper bound of the asymptotic variance Since η is the limit of

$$(T-L+1)^{-1} \sum_{t=L}^T \text{Var}\{[\xi_t(F^2, L) - \xi_t(F^1, L)]N(Y_t, B) \mid \bar{H}_{t-L}^*\},$$

we cannot directly estimate η from the data without additional assumptions (available data are on a single time series and we do not have access to replicates of the world with respect to $W_{t-L+1}, M_{t-L+1} \dots, W_t$ given \bar{H}_{t-L}^*). Instead, we consider

$$\eta_t^* = E\left\{ \left\{ [\xi_t(F^2, L) - \xi_t(F^1, L)]N(Y_t, B) \right\}^2 \mid \bar{H}_{t-L}^* \right\} \geq \eta_t$$

for which

$$(T-L+1)^{-1} \sum_{t=L}^T \eta_t^* \rightarrow \eta^* \geq \eta.$$

We show that $\hat{\eta}^* = (T-L+1)^{-1} \sum_{t=L}^T \left[\widehat{\tau}_{Bt}(F', F'', L) \right]^2$ is a consistent estimator for η^* , by showing that

1. $\hat{\eta}^* = (T-L+1)^{-1} \sum_{t=L}^T \left\{ [\xi_t(F^2, L) - \xi_t(F^1, L)]N(Y_t, B) \right\}^2$ is consistent for η^* , and
2. $\hat{\eta}^* - \tilde{\eta}^* \xrightarrow{p} 0$.

Define $\Psi_t = \left\{ [\xi_t(F^2, L) - \xi_t(F^1, L)]N(Y_t, B) \right\}^2 - \eta_t^*$. Then, Ψ_t is a martingale difference series with respect to \bar{H}_{t-L+1}^* since the following two hold:

- $E(|\Psi_t|) < \infty$ since Ψ_t is bounded (derived using Assumption 4 and Assumption S.1(a)), and
- $E(\Psi_t \mid \bar{H}_{t-L+1}^*) = E\left\{ [\xi_t(F^2, L) - \xi_t(F^1, L)]N(Y_t, B) \mid \bar{H}_{t-L}^* \right\} - \eta_t^* = 0$.

Also, since $[\xi_t(F^2, L) - \xi_t(F^1, L)]N(Y_t, B)$ is bounded we have that $\sum_{t=L}^{\infty} t^{-2}E(\Psi_t^2) < \infty$. From Theorem 1 in Csörgö (1968) we have that

$$\frac{1}{T-L+1} \sum_{t=L}^T \Psi_t = \frac{1}{T-L+1} \sum_{t=L}^T \{[\xi_t(F^2, L) - \xi_t(F^1, L)]N(Y_t, B)\}^2 - \frac{1}{T-L+1} \sum_{t=L}^T \eta_t^* \xrightarrow{p} 0,$$

showing that $\tilde{\eta}^*$ consistently estimates the asymptotic variance bound η^* . Next, write

$$\begin{aligned} \hat{\eta}^* - \tilde{\eta}^* &= (T-L+1)^{-1} \sum_{t=L}^T [\xi_t(F^2, L) - \xi_t(F^1, L)]^2 \{N(\tilde{Y}_t, B)^2 - N(Y_t, B)^2\} \\ &= (T-L+1)^{-1} \sum_{t=L}^T [\xi_t(F^2, L) - \xi_t(F^1, L)]^2 \{N(\tilde{Y}_t, B) + N(Y_t, B)\} \{N(\tilde{Y}_t, B) - N(Y_t, B)\} \\ &= (T-L+1)^{-1} \sum_{t=L}^T c_t \{N(\tilde{Y}_t, B) - N(Y_t, B)\} \end{aligned}$$

for $c_t = [\xi_t(F^2, L) - \xi_t(F^1, L)]^2 \{N(\tilde{Y}_t, B) + N(Y_t, B)\}$. Note that since $\xi_t(F, L)$ is bounded (using Assumption 4) and since $N(\tilde{Y}_t, B), N(Y_t, B)$ are bounded (using Assumption S.1(a)), the constants c_t are also bounded. Therefore, following the proof for convergence to zero of the second error q_{2Bt} , we can show that $\sqrt{T}(\hat{\eta}^* - \tilde{\eta}^*) \xrightarrow{p} 0$ which of course implies that $\hat{\eta}^* - \tilde{\eta}^* \xrightarrow{p} 0$. Therefore, $\hat{\eta}^*$ is consistent for η^* . □

B.3 Theorem 2: Asymptotic normality for estimator within d -neighborhood

Estimand and estimator within d -neighborhood In addition to the main causal estimands and estimators defined in the manuscript, we hereby define additional causal quantities of interest related to the local spatial spillover effects of airstrikes. In particular, we consider the expected number of outcome active locations during time period t within distance d of each airstrike that would occur over the previous l time periods under the scenario that the distribution of treatment and mediator were to be set to F over the preceding $L \geq l$ time periods. Note that the number of time periods over which the intervention takes place, L , does not have to equal the number of time periods whose treatment neighborhoods we consider, l .

Formally, this estimand is defined as,

$$N_{ldt}(F, L) = \int_{(\mathcal{W}, \mathcal{M})^L} N_{\mathcal{N}_{ldt}}(Y_t(\overline{\mathbf{W}}_{t-L}, \overline{\mathbf{M}}_{t-L}, w_{t-L+1}, m_{t-L+1}, \dots, w_t, m_t)) \prod_{t'=t-L+1}^t dF(w_{t'}, m_{t'}). \quad (22)$$

where \mathcal{N}_{ldt} represents the collection of neighborhoods within distance d of all treatment active locations during the last l time periods, i.e., $\mathcal{N}_{ldt} = \{\omega \in \Omega : \text{dist}(s, \omega) < d \text{ for some } s \in \bigcup_{t'=t-l+1}^t S_{W_{t'}}\}$. Note that for simplicity we suppress the dependence of \mathcal{N}_{ldt} on W_{t-l+1}, \dots, W_t in our notation.

Although the form of \mathcal{N}_{ldt} resembles that of \mathcal{N}_{Bt} , these two quantities critically differ in that while the set \mathcal{N}_{ldt} depends on the treatment active locations, (w_{t-l+1}, \dots, w_t) , while B does not. This means that a greater number of previous treatment active locations directly leads to a greater number of value of \mathcal{N}_{ldt} . Therefore, we may standardize the quantity in equation (22) by the area of \mathcal{N}_{ldt} . We define the expected *rate* of outcome active locations per areal unit according to F as

$$\mathbf{N}_{ldt}^*(F, L) = \int_{(\mathcal{W}, \mathcal{M})^L} N_{\mathcal{N}_{ldt}}(Y_t(\overline{\mathbf{W}}_{t-L}, \overline{\mathbf{M}}_{t-L}, w_{t-L+1}, m_{t-L+1}, \dots, w_t, m_t)) / \alpha(\mathcal{N}_{ldt}) \prod_{t'=t-L+1}^t dF(w_{t'}, m_{t'}), \quad (23)$$

where $\alpha(\mathcal{N}_{ldt})$ represents the area of the set \mathcal{N}_{ldt} .

We cannot consistently estimate the causal estimands defined above for a specific time period t since for every time period we have only one realization of the treatment, mediator, and outcome point patterns. Thus, we consider the following temporal average of the causal estimands,

$$\mathbf{N}_{ld}(F, L) = \frac{1}{T - L + 1} \sum_{t=L}^T \mathbf{N}_{Bt}(F, L), \quad (24)$$

$$\mathbf{N}_{ld}^*(F, L) = \frac{1}{T - L + 1} \sum_{t=L}^T \mathbf{N}_{ldt}^*(F, L). \quad (25)$$

Using these estimands, we can compare two stochastic interventions, $F' = (F'_W, F'_{M|w})$, and $F'' = (F''_W, F''_{M|w})$. We define the temporal average causal effect of a change in the intervention distribution from F' to F'' over the previous L time periods as the following contrasts,

$$\tau_{ld}^*(F', F'', L) = \mathbf{N}_{ld}^*(F'', L) - \mathbf{N}_{ld}^*(F', L), \quad (26)$$

The causal effect τ_B describes the change in the expected number of outcome active locations within region B if the treatment and mediator distribution during the last L time periods were changed from F' to F'' . The causal effect τ_{ld}^* describes how the same change in the intervention distribution affects the outcome response nearby the treatment active locations. By comparing this estimand across different values of d , researchers can evaluate the distance at which spatial spillover effects attenuate. However, this estimand should be interpreted with care. For any given values of l , d , and t , this causal effect may arise either because the two interventions yield different number of treatment active locations or because they produce different neighborhoods \mathcal{N}_{ldt} . This is the reason why we do not consider the contrast with

respect to $N_{ld}(F, L)$, which is not a standardized quantity.

We should notice that using the smoothed outcome $N(\tilde{Y}_t, B)$ is less important when estimating quantities that are defined over a pre-specified region, and for which visualizations as a function of space are not applicable. Estimands that are defined in terms of d -neighborhoods of previous treatments belong to this category, since the set \mathcal{N}_{ldt} is not a fixed subset of Ω . For such estimands, the estimators below are defined in terms of $N(Y_t, \mathcal{N}_{ldt})$ directly, where with some abuse of notation, we use \mathcal{N}_{ldt} to denote the d -neighborhoods of the *observed* treatment active locations at time periods $t - l + 1, \dots, t$. Specifically, we define the estimator of the expected number of points within distance d of the past l treatment active locations as

$$\widehat{N}_{ld}(F, L) = \frac{1}{T - L + 1} \sum_{t=L}^T \xi_t(F, L) N(Y_t, \mathcal{N}_{ldt}), \quad (27)$$

and the estimator of the rate of outcome active locations within distance d as

$$\widehat{N}_{ld}^*(F, L) = \frac{1}{T - L + 1} \sum_{t=L}^T \frac{\xi_t(F, L)}{\alpha(\mathcal{N}_{ldt})} N(Y_t, \mathcal{N}_{ldt}). \quad (28)$$

Based on these estimators, estimators for τ_{ld} , τ_{ld}^{DE} and τ_{ld}^{IE} are defined as

$$\begin{aligned} \widehat{\tau}_{ld}(F', F'', L) &= \widehat{N}_{ld}(F'', L) - \widehat{N}_{ld}(F', L), \\ \widehat{\tau}_{ld}^{\text{DE}}(F'_W, F''_W; L, F_{M|w}) &= \widehat{\tau}_{ld}((F'_W, F_{M|w}), (F''_W, F_{M|w}), L), \\ \widehat{\tau}_{ld}^{\text{IE}}(F'_{M|w}, F''_{M|w}; L, F_W) &= \widehat{\tau}_{ld}((F_W, F'_{M|w}), (F_W, F''_{M|w}), L), \end{aligned} \quad (29)$$

and similarly for $(\tau_{ld}^*, \tau_{ld}^{*\text{DE}}, \tau_{ld}^{*\text{IE}})$ and $(\tau_{ld}^{\text{SS}}, \tau_{ld}^{\text{SS,DE}}, \tau_{ld}^{\text{SS,IE}})$.

The asymptotic properties for these estimators are derived separately because (a) the estimators use the outcome Y_t directly instead of the smoothed outcome \tilde{Y}_t , and (b) all quantities involve the set \mathcal{N}_{ldt} which is a set of locations in Ω which changes over different draws from the intervention in the definition of the estimands. These modifications are addressed in the following theorem:

Theorem 2 (Asymptotic normality for estimators of d -neighborhood estimands). *If Assumption 4 and the regularity conditions in the appendix hold, then*

$$\begin{aligned} \sqrt{T}(\widehat{\tau}_{ld}(F', F'', L) - \tau_{ld}(F', F'', L)) &\xrightarrow[T \rightarrow \infty]{d} N(0, \eta_{ld}) \\ \sqrt{T}(\widehat{\tau}_{ld}^*(F', F'', L) - \tau_{ld}^*(F', F'', L)) &\xrightarrow[T \rightarrow \infty]{d} N(0, \eta_{sld}). \end{aligned}$$

Furthermore, upper bounds of the variances η_{ld} , η_{sld} and η_{ld}^{SS} can be consistently estimated by

$$(T - L + 1)^{-1} \sum_{t=L}^T \left[\widehat{\tau}_{ldt}(F', F'', L) \right]^2,$$

$$(T - L + 1)^{-1} \sum_{t=L}^T \left[\widehat{\tau}_{ldt}^*(F', F'', L) \right]^2$$

respectively.

The result of Theorem 2 also holds for the estimators in (27) and (28) of the expected number and the expected rate, respectively, of outcome events within distance d of previous treatments. Theorem 2 also establishes the asymptotic normality of estimators of the *direct and indirect effects* of the treatment point pattern on the outcome near previous treatment active locations, and the direct and indirect effects of the treatment on the locality of the outcome response. In contrast to Theorem 1, Theorem 2 does not require a shrinking bandwidth parameter since the outcome Y_t is used directly.

Proof of Theorem 2.

Asymptotic normality for estimator within d -neighborhood Write

$$\begin{aligned} e_{ldt} &= \widehat{\tau}_{ldt}(F', F'', L) - \tau_{ldt}(F', F'', L) \\ &= \widehat{\mathbf{N}}_{ldt}(F'', L) - \widehat{\mathbf{N}}_{ldt}(F', L) - \left[\mathbf{N}_{ldt}(F'', L) - \mathbf{N}_{ldt}(F', L) \right] \\ &= [\xi_2(F, L) - \xi_1(F, L)] N(Y_t, \mathcal{N}_{ldt}) - \left[\mathbf{N}_{ldt}(F'', L) - \mathbf{N}_{ldt}(F', L) \right] \end{aligned}$$

Like in the proof of Theorem 1, we show that e_{ldt} is a martingale difference series with respect to \overline{H}_{t-L}^* by showing that $E(|e_{ldt}|) < \infty$ and $E(e_{ldt} \mid \overline{H}_{t-L}^*) = 0$, and that for every $\epsilon > 0$, $(T - L + 1)^{-1} \sum_{t=L}^T E\{e_{ldt}^2 I(|e_{ldt}| > \epsilon \sqrt{T - L + 1}) \mid \overline{H}_{t-L}^*\} \xrightarrow{P} 0$. Then we use Theorem 4.16 of van der Vaart (2010) to get asymptotic normality.

Clearly, from Assumptions 4 and S.1(a) and following steps similar to the ones in (19), we have that $|e_{ldt}| \leq 2\delta_Y(\delta_W^L \delta_M^L + 1)$ which shows that $E(|e_{ldt}|) \leq \infty$. Then, for the T_0 value in (21), we also have that for $T > T_0$, $E(e_{ldt}^2 I(|e_{ldt}| > \epsilon \sqrt{T - L + 1}) \mid \overline{H}_{t-L}^*) = 0$. So it suffices to show that $E(e_{ldt} \mid \overline{H}_{t-L}^*) = 0$. Following steps similar to (20), we can show that

$$E \left[\xi_t(F, L) N(Y_t, \mathcal{N}_{ldt}) \mid \overline{H}_{t-L}^* \right] = \mathbf{N}_{ldt}(F, L),$$

by noticing that the dependence of the neighboring set \mathcal{N}_{ldt} on previous treatments is averaged over according to the stochastic intervention when we consider the estimator's expectation. Therefore, the

conditions are shown, and from Theorem 4.16 of [van der Vaart \(2010\)](#) we have that, if

$$(T - L + 1)^{-1} \sum_{t=L}^T \eta_{ldt} \xrightarrow{p} \eta_{ld},$$

for some $\eta_{ld} \in \mathbb{R}^+$, where $\eta_{ldt} = \text{Var}\{[\xi_t(F^2, L) - \xi_t(F^1, L)]N(Y_t, \mathcal{N}_{ldt}) \mid \overline{H}_{t-L}^*\}$ (adaptation of Assumption S.1(b)), then

$$\sqrt{T}(\widehat{\tau}_{ld}(F', F'', L) - \tau_{ld}(F', F'', L)) \xrightarrow[T \rightarrow \infty]{d} N(0, \eta_{ld}).$$

We can again use [Csörgő \(1968\)](#) and the estimator's boundedness to show that

$$(T - L + 1)^{-1} \sum_{t=L}^T \left\{ \left[\widehat{\tau}_{ldt}(F', F'', L) \right]^2 - \eta_{ldt}^* \right\} \xrightarrow{p} 0,$$

where $\eta_{ldt}^* = E\left\{ \left\{ [\xi_t(F^2, L) - \xi_t(F^1, L)]N(Y_t, \mathcal{N}_{ldt}) \right\}^2 \mid \overline{H}_{t-L}^* \right\} \geq \eta_{ldt}$.

Asymptotic normality for rate estimator within d -neighborhood Write

$$\begin{aligned} e_{ldt}[s] &= \widehat{\tau}_{ldt}^*(F', F'', L) - \tau_{ldt}^*(F', F'', L) \\ &= \widehat{\mathbf{N}}_{ldt}^*(F'', L) - \widehat{\mathbf{N}}_{ldt}^*(F', L) - \left[\mathbf{N}_{ldt}^*(F'', L) - \mathbf{N}_{ldt}^*(F', L) \right] \\ &= \frac{\xi_2(F, L) - \xi_1(F, L)}{\alpha(\mathcal{N}_{ldt})} N(Y_t, \mathcal{N}_{ldt}) - \left[\mathbf{N}_{ldt}^*(F'', L) - \mathbf{N}_{ldt}^*(F', L) \right], \end{aligned} \tag{30}$$

This proof follows similarly, with minor modifications. For example, we can show that

$$|e_{ldt}[s]| \leq 2\delta_Y(\delta_W^L \delta_M^L / \alpha(\Omega) + 1),$$

which shows that $E(|e_{ldt}[s]|) < \infty$. By choosing the value of T_0 following the steps in (21) for this bound, we have that $E(e_{ldt}^2 I(|e_{ldt}| > \epsilon \sqrt{T - L + 1}) \mid \overline{H}_{t-L}^*) = 0$ for $T \geq T_0$. Lastly, $E(e_{ldt}[s] \mid \overline{H}_{t-L}^*) = 0$ follows similarly to $E(e_{ldt} \mid \overline{H}_{t-L}^*) = 0$, where again the dependence of the estimator and estimand on \mathcal{N}_{ldt} is addressed by averaging over the treatment values that define \mathcal{N}_{ldt} . By assuming that

$$(T - L + 1)^{-1} \sum_{t=L}^T \eta_{ldt}[s] \xrightarrow{p} \eta_{sld},$$

for some $\eta_{sld} \in \mathbb{R}^+$, where $\eta_{ldt}[s] = \text{Var}\{\widehat{\tau}_{ldt}^*(F', F'', L) \mid \overline{H}_{t-L}^*\}$, we have that

$$\sqrt{T}(\widehat{\tau}_{ld}^*(F', F'', L) - \tau_{ld}^*(F', F'', L)) \xrightarrow[T \rightarrow \infty]{d} N(0, \eta_{sld}),$$

and $(T - L + 1)^{-1} \sum_{t=L}^T [\widehat{\tau}_{ldt}(F', F'', L)]^2$ consistently estimates an upper bound of the asymptotic variance since

$$(T - L + 1)^{-1} \sum_{t=L}^T \left\{ \left[\widehat{\tau}_{ldt}(F', F'', L) \right]^2 - E \left\{ \left[\widehat{\tau}_{ldt}^*(F', F'', L) \right]^2 \mid \overline{H}_{t-L}^* \right\} \right\} \xrightarrow{p} 0.$$

Asymptotic normality for effect estimator on spatial spillover Write

$$\begin{aligned} e_{ldt}^{SS} &= \widehat{\tau}_{ldt}^{SS}(F', F'', L) - \tau_{ldt}^{SS}(F', F'', L) \\ &= \widehat{SS}_{ldt}(F'', L) - \widehat{SS}_{ldt}(F', L) - \left[SS_{ldt}(F'', L) - SS_{ldt}(F', L) \right] \\ &= [\xi_2(F, L) - \xi_1(F, L)] \left[|S_{Y_t}| - \frac{\alpha(\Omega)}{\alpha(\mathcal{N}_{ldt})} N(Y_t, \mathcal{N}_{ldt}) \right] - \\ &\quad \left\{ \left[\mathbf{N}_{\Omega t}(F'', L) - \alpha(\Omega) \cdot \mathbf{N}_{ldt}^*(F'', L) \right] - \left[\mathbf{N}_{\Omega t}(F', L) - \alpha(\Omega) \cdot \mathbf{N}_{ldt}^*(F', L) \right] \right\} \\ &= \left\{ [\xi_2(F, L) - \xi_1(F, L)] |S_{Y_t}| - \left[\mathbf{N}_{\Omega t}(F'', L) - \mathbf{N}_{\Omega t}(F', L) \right] \right\} - \\ &\quad \alpha(\Omega) \left\{ \frac{\xi_2(F, L) - \xi_1(F, L)}{\alpha(\mathcal{N}_{ldt})} N(Y_t, \mathcal{N}_{ldt}) - \left[\mathbf{N}_{ldt}^*(F'', L) - \mathbf{N}_{ldt}^*(F', L) \right] \right\} \\ &= q_{1\Omega t} - e_{ldt}[s], \end{aligned}$$

where $q_{1\Omega t}$ is defined in (18) and $e_{ldt}[s]$ is defined in (30). Since $q_{1\Omega t}$ and $e_{ldt}[s]$ are bounded with expectations conditional on \overline{H}_{t-L}^* equal to 0, we only need to assume that

$$(T - L + 1)^{-1} \sum_{t=L}^T \eta_{ldt}^{SS} \xrightarrow{p} \eta_{ld}^{SS}$$

for asymptotic normality, for some $\eta_{ld}^{SS} \in \mathbb{R}^+$, and $\eta_{ldt}^{SS} = \text{Var} \{ \widehat{\tau}_{ldt}^{SS}(F', F'', L) \mid \overline{H}_{t-L}^* \}$. Then

$$\sqrt{T} (\widehat{\tau}_{ld}^{SS}(F', F'', L) - \tau_{ld}^{SS}(F', F'', L)) \xrightarrow[T \rightarrow \infty]{d} N(0, \eta_{ld}^{SS}),$$

and $(T - L + 1)^{-1} \sum_{t=L}^T \left[\widehat{\tau}_{ldt}^{SS}(F', F'', L) \right]^2$ consistently estimates an upper bound of the asymptotic variance. □

C Average treatment effects

C.1 Estimation of propensity scores

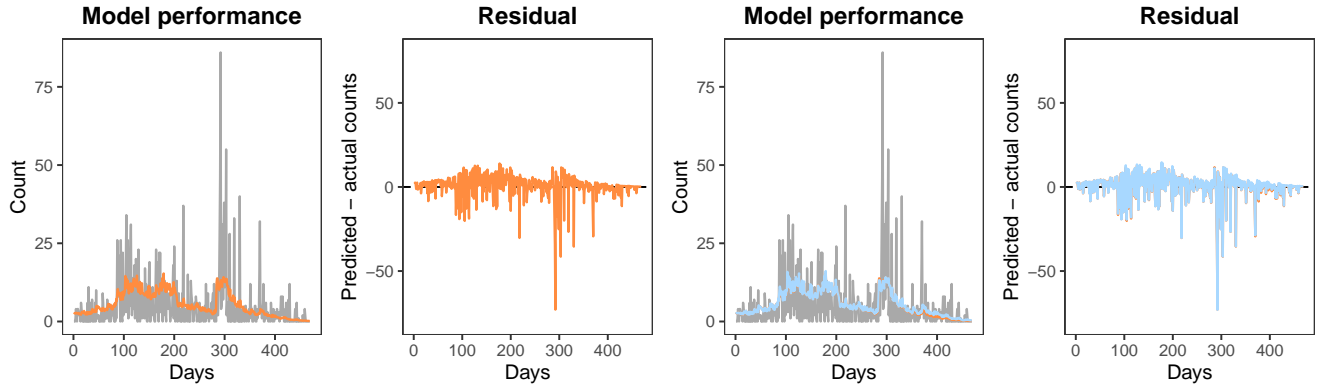


Figure S1: **Model performance.** The first panel (left, model performance) shows the actual and predicted counts (in gray and orange, respectively), and the second panel shows the residual plot. The third and fourth panels do the same with the first 80% of observations to examine out-of-sample prediction performance.

C.2 Estimation of causal effects

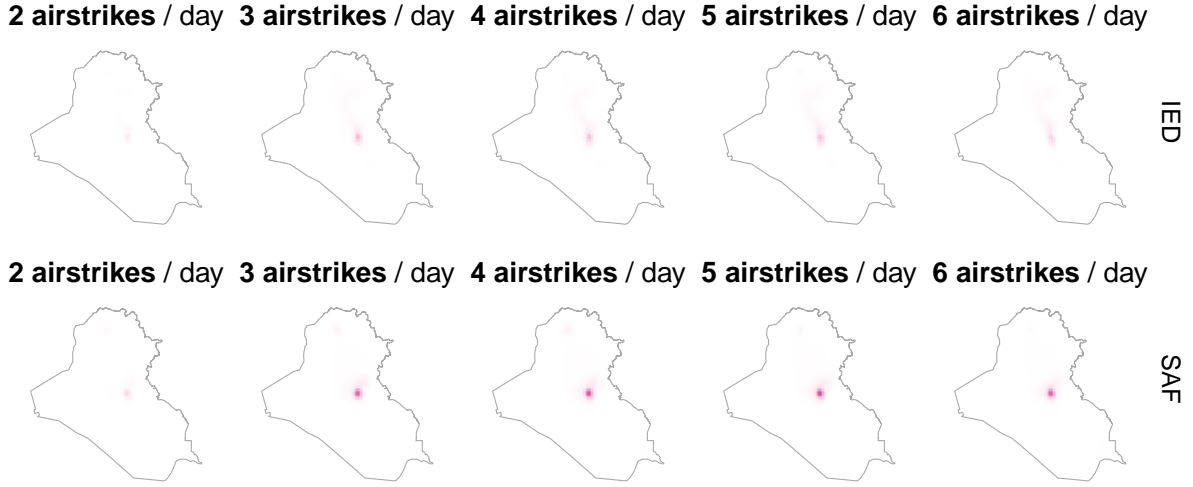


Figure S2: **Differences in outcome surfaces for intensity changes.** The first and second rows correspond to IED and SAF, respectively (with $L = 10$). The areas in red and blue exhibit those with increased and decreased intensities of insurgent activities, respectively.

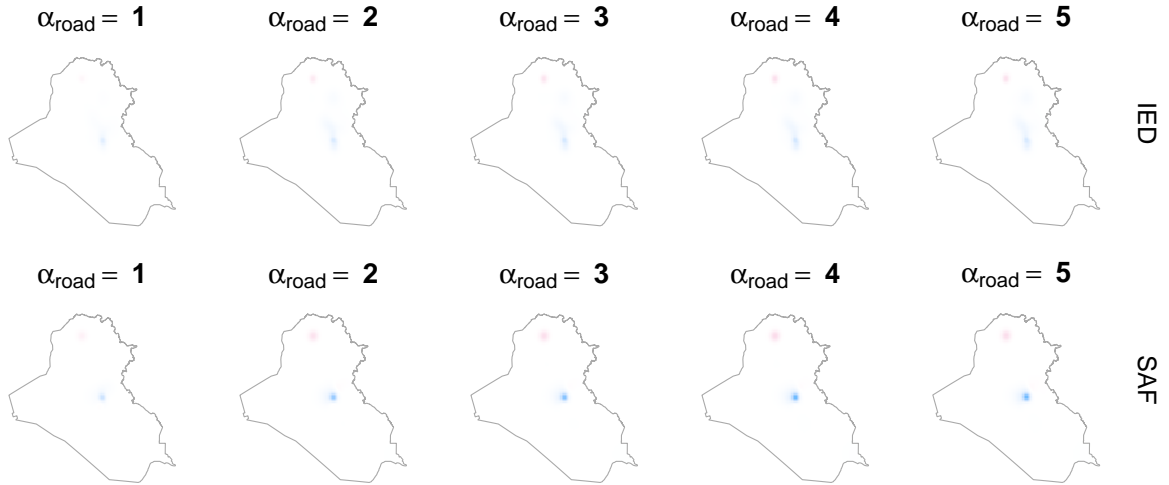


Figure S3: **Differences in outcome surfaces for location shifts.** The first and second rows correspond to IED and SAF, respectively (with $L = 10$). The areas in red and blue exhibit those with increased and decreased intensities of insurgent activities, respectively.

D Heterogeneous treatment effects

D.1 Troop characteristics

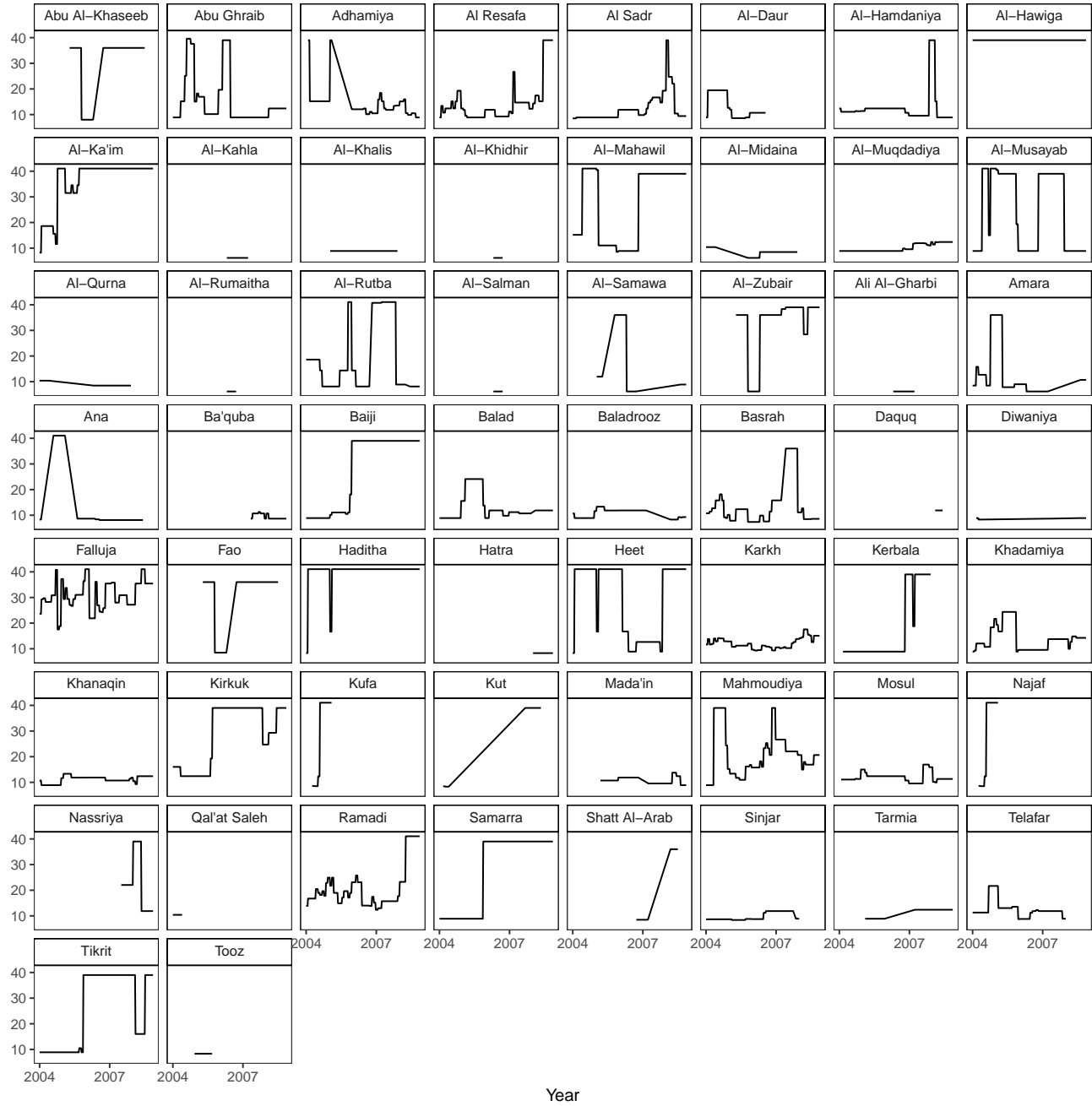


Figure S4: **Troop characteristics: Mechanization.** Weekly-level data from all districts are displayed.

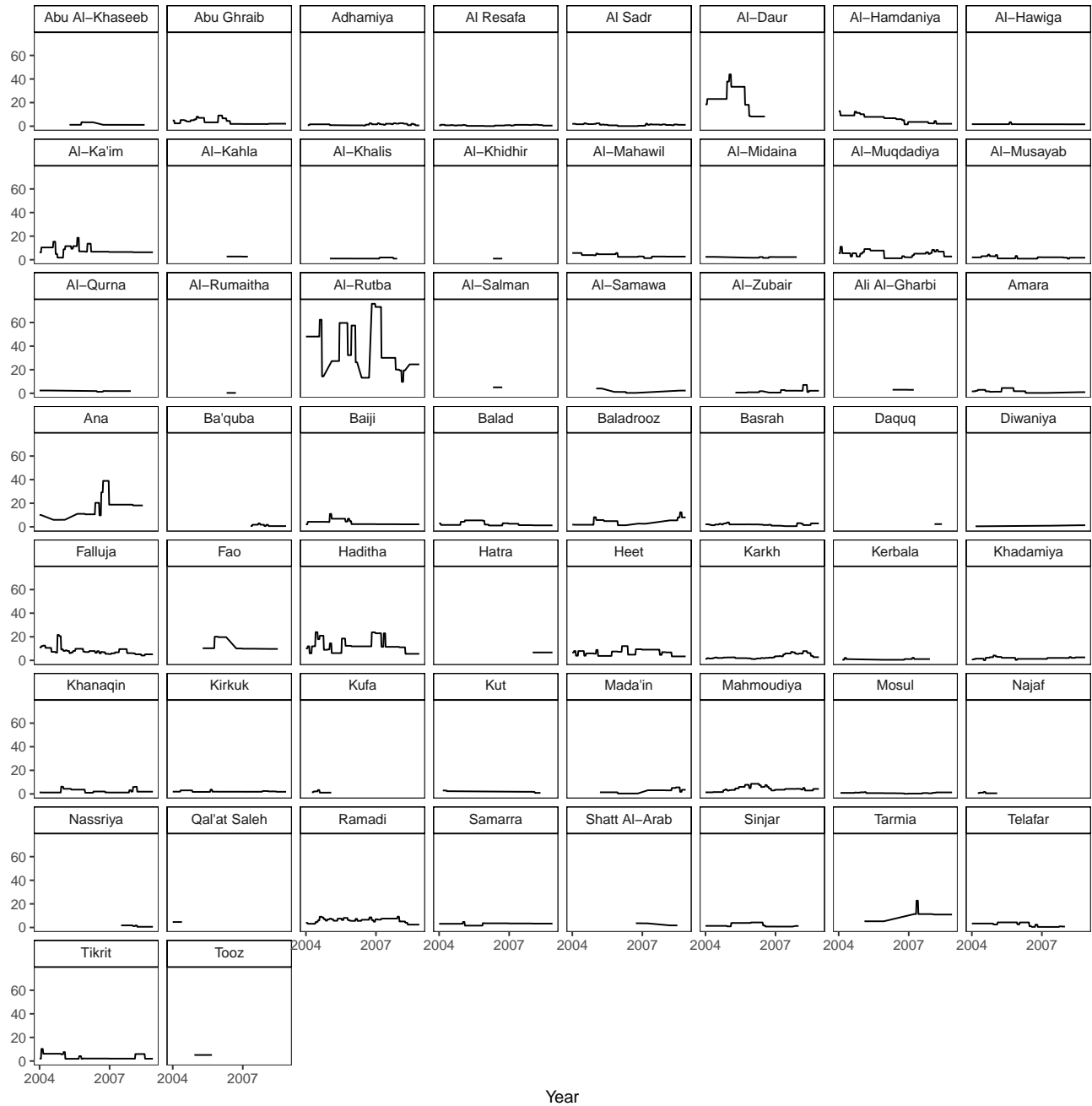


Figure S5: **Troop characteristics: Troop density.** Weekly-level data from all districts are displayed.

E Causal mediation analysis

E.1 Model fit

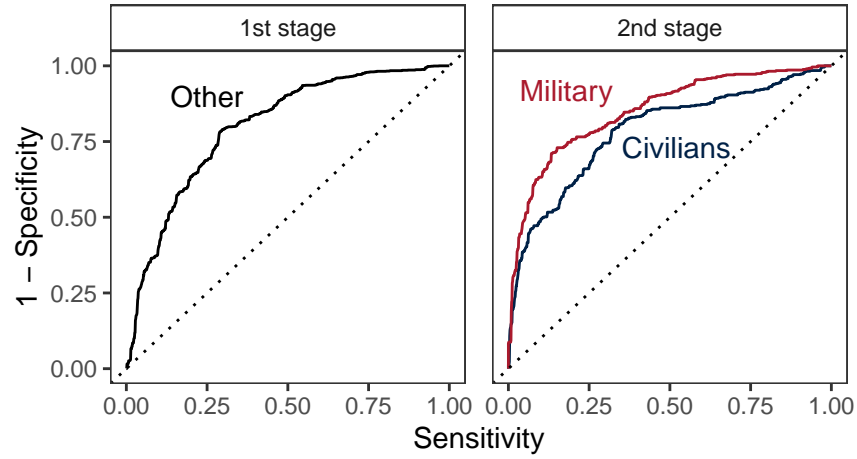


Figure S6: **Receiver operating characteristic curves (ROCs).** The left panel shows the ROC curve for the first stage, and the right panel shows the ROC curves for the second stage (civilians and military targets in blue and red, respectively). The areas under the curve (AUCs) are 0.796 for the first stage, 0.781 for the second stage (civilians), and 0.851 for the second stage (military targets). The 45-degree lines are shown as dotted lines.

E.2 Main results in other geographical areas

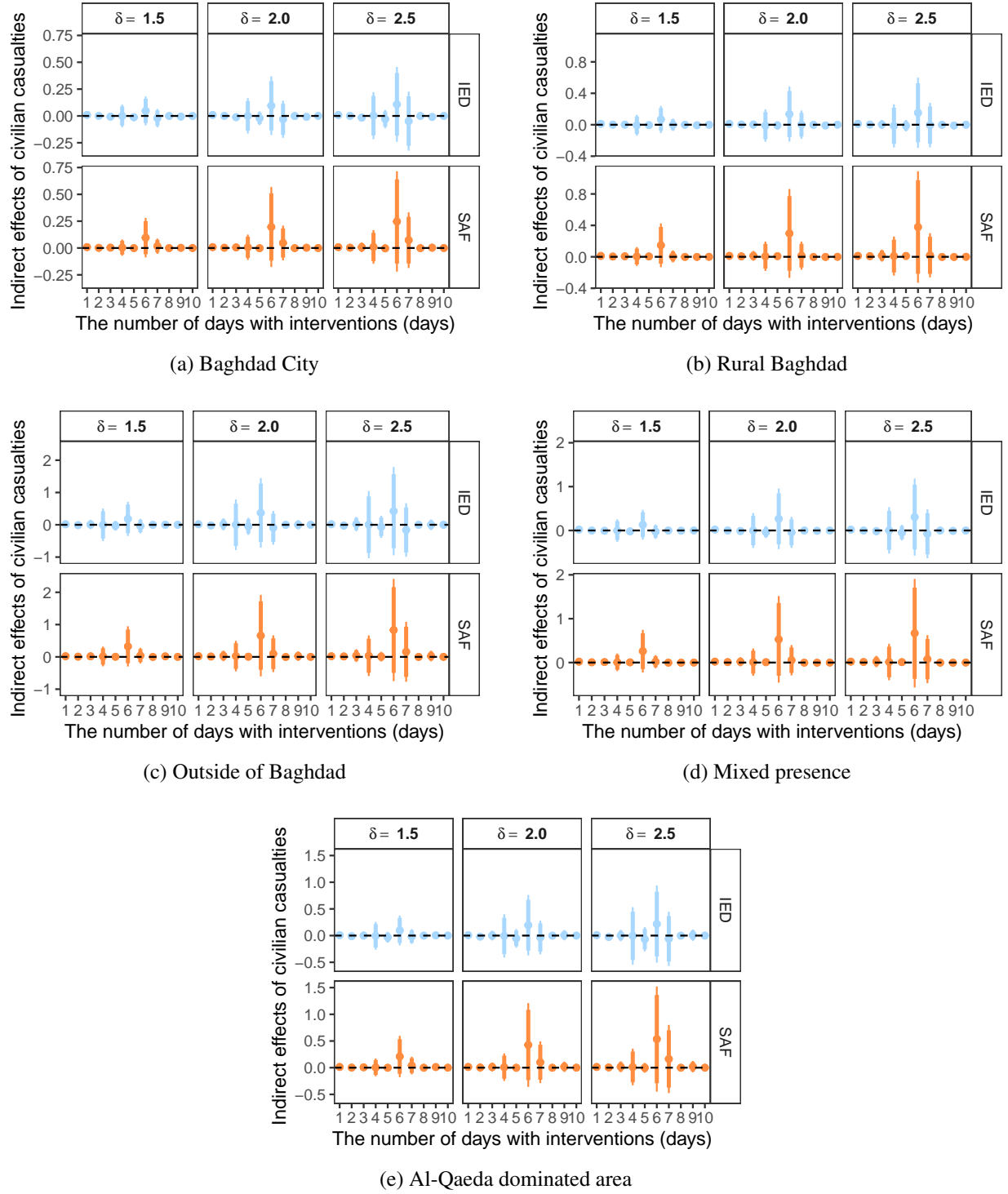


Figure S7: **Indirect effects of civilian casualties in other areas.** Indirect effects in (a) Baghdad City, (b) rural Baghdad, (c) outside Baghdad, (d) areas with Sunni/Shia mixed presence, and (e) Al-Qaeda dominated areas are shown.

E.3 Main results using an indicator for civilian casualties

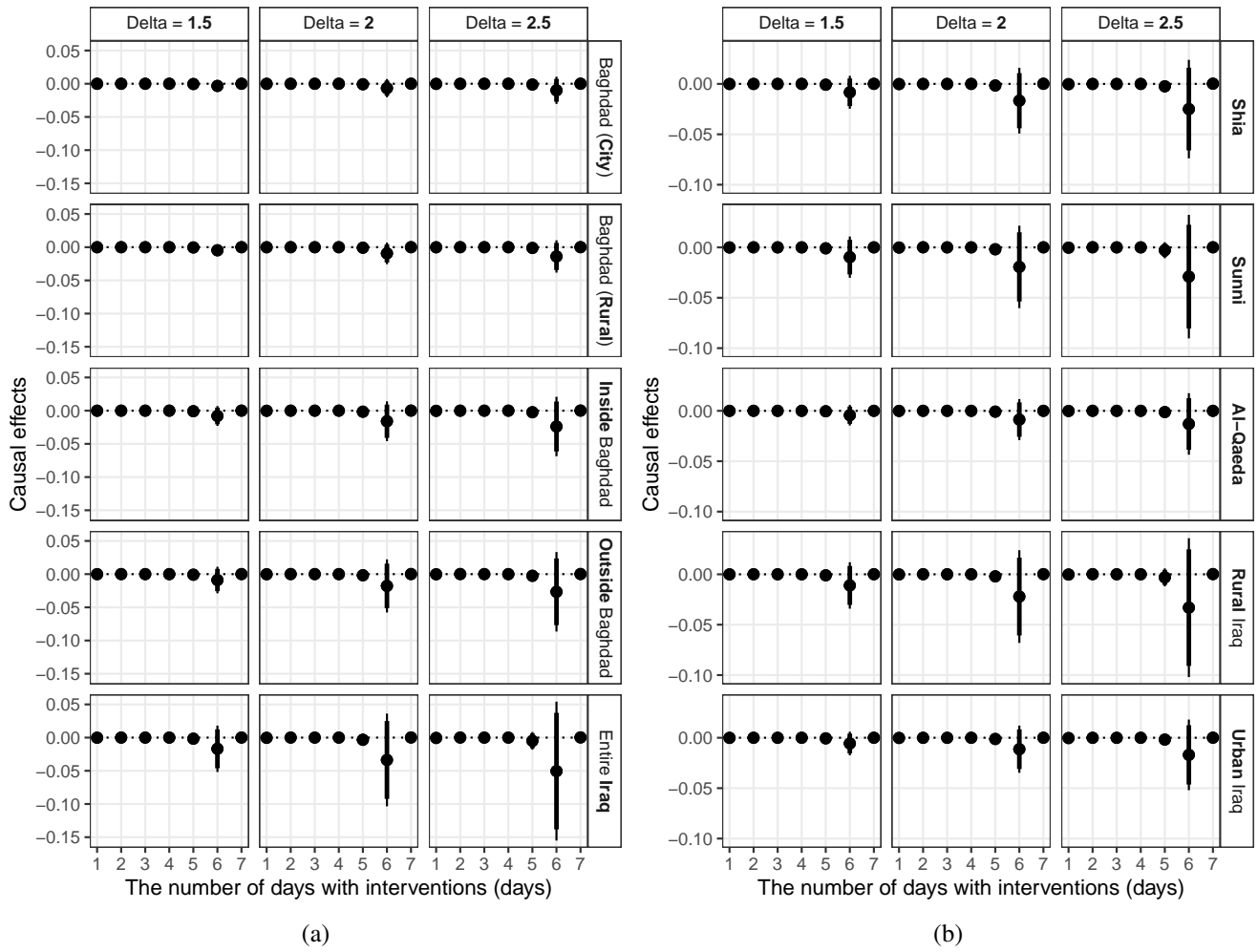


Figure S8: **Indirect effects of civilian casualties based on the binary civilian casualty variable.** In all geographical and politically salient areas, we do not observe significant indirect effects.